46th AIAA Aerospace Sciences Meeting and Exhibit
7 - 10 January 2008, Reno, Nevada

AIAA 2008-501

Hypersonic Boundary-Layer Transition on Blunt Bodies with Roughness*

Steven P. Schneider†
School of Aeronautics and Astronautics
Purdue University
West Lafayette, IN 47907-1282

Abstract

Laminar-turbulent transition on the Crew Exploration Vehicle (CEV, or Orion) is likely to be dominated by the effects of ablation and the laminar-ablated roughness, both isolated and distributed. Although no single ground experiment can simultaneously duplicate all aspects of this complex process, many experiments have been carried out using roughness applied to non-porous models without blowing. The present document reviews these data for the effect of roughness on hypersonic blunt-body transition. A few experiments have also looked at cold gases blown through a rough wall to simulate the flow due to ablation. Although these effects of ablation are critical and may in fact be dominant, they are to be reviewed later.

Introduction

Laminar-turbulent transition in hypersonic boundary layers is important for prediction and control of heat transfer, skin friction, and other boundary layer properties. Vehicles that spend extended periods at hypersonic speeds may be critically affected by the uncertainties in transition prediction, depending on their Reynolds numbers. However, the mechanisms leading to transition are still poorly understood, even in low-noise environments. These mechanisms include the concave-wall Görtler instability [1], the first and second mode streamwise-instability waves described by Mack [2], and the 3D crossflow instability [3, 4].

Nearly all hypersonic ground-test facilities suffer from high levels of noise radiated from the turbulent boundary layers on the nozzle walls. The effect of this noise on transition is often poorly understood, although it has been an issue for more than 50 years [5]. For roughness elements that are less than 'effective', so transition occurs well downstream of the roughness, tunnel noise has been shown to have a substantial effect [6, 7]. Quiet tunnels with laminar nozzle-wall boundary layers have been developed to provide low noise levels comparable to flight, but quiet-tunnel research has been very limited to date [8].

The present review was developed for analyzing boundary-layer transition on the Orion or CEV, a manned NASA reentry vehicle that is very similar to Apollo. The author has earlier reviewed transition on reentry capsules and planetary probes [9]. See also the other transition issues reviewed in Refs. [6, 10, 11]. An overall review of roughness effects on hypersonic transition was reported in Ref. [12]. The reader is encouraged to study Ref. [12] as an introduction to the present paper; the extensive introduction in that reference will not be repeated here. Earlier reviews of roughness effects on blunt bodies include those of Reda [13, 14] and Batt and Legner [15]. Berry and Horvath recently reviewed NASA-Langley measurements of transition induced by discrete roughness, along with recent flight data from the Space Shuttle [16]. Ref. [16] describes work on slender vehicles like the X-43A, moderately blunt vehicles like the Shuttle, and blunt vehicles like planetary probes, but only the latter are reviewed in the present paper. The present paper also reviews some additional smooth-wall aeroheating data that was located after the completion of Ref. [9].

Transition on Apollo-like shapes is affected by the chemistry and massflow of the gases blown from the ablating thermal protection system (TPS). It is also affected by the surface roughness of the laminar ablated TPS. This is a complex problem which was comprehensively researched in the 1960's and 1970's. However, the area then fell out of favor, little has been done since the 1980's, and few of the earlier researchers are still available for comment. The author has worked almost exclusively on tran-

*AIAA Paper 2008-0501, presented at the Jan. 2008 Aerospace Sciences Meeting

†Professor. Associate Fellow, AIAA.

sition since 1985, and on high-speed transition since 1990, but even a 7500-paper library and database is far from complete; the author still has much to learn about the vast literature for high-speed transition. Since 2004, with the interest in the impending CEV, a significant proportion of the author's effort has gone towards reviewing the literature in this area, but this work is far from complete. The present review is mainly focused on surface roughness effects.

The laminar-ablated Orion will contain two different kinds of surface roughness: (1) isolated roughness due to the compression pads, possible TPS joints, and other localized nonuniformities, and (2) distributed roughness due to the laminar ablated TPS surface. The relevant literature comes from two main sources: (1) NASA-funded research in support of Mercury, Gemini, Apollo, and the planetary probes, some of which is reviewed in Ref. [9], and (2) DoD-funded research studying transition on the blunt nosetips of reentry vehicles. The problem is complex, so most of the useful literature describes flight tests and experimental studies in ground facilities, since the computational methods available when the earlier work was done were generally primitive. These experiments are very expensive to carry out or repeat, and the budget and schedule of the Orion will only permit an effort which is much less comprehensive than the Cold War studies. Thus, the author believes it is cost-effective to comprehensively review these earlier studies in order to identify experiments worthy of reanalysis with modern computational methods, and to better plan and analyze the new experiments that should be carried out.

At present, the Orion is being designed using turbulent heating [16]. Isolated roughness at the service-module attachment points has been an issue, but at present these are to be designed so they are retractable. Although transition is not currently a primary issue for the Orion design, it appears likely to arise later, as mass becomes more critical, analyses attempt to become more accurate and reliable, and more off-design conditions are analyzed.

Additional Smooth-Wall Aero-Heating Data for Apollo

Apparently Laminar Data

Following the completion of Ref. [17], which became Ref. [9], additional aeroheating data was located. Since this aeroheating data had the potential to supply additional information regarding transition on Apollo, it is summarized here. However, so far all the data in this section appear to be laminar.

Tunnel C heat-transfer measurements with Apollo model H-1 are reported in Ref. [18]. All measurements were on a smooth-wall model. These Mach-10 measurements were carried out at zero angle of attack. The Reynolds number based on freestream conditions and diameter ranged from $0.616 - 1.480 \times 10^6$. There was apparently a problem with nonuniformity of the tunnel centerline flow, as determined by comparisons to Lee's laminar theory. However, it appears that the data are all laminar.

Apollo aeroheating measurements were also obtained in a shock tunnel at Ames at high enthalpy [19]. The Mach number was 10 and the angles of attack ranged from 0 to 44 deg. However, the Reynolds number was only 60,000/ft. in the freestream, with models that were 2.5-in. diameter, and the data are apparently all laminar. Afterbody separation began near 23-deg. AOA, while the flow over most of the windward surface was attached at 33-deg. AOA.

Miller et al. measured heat transfer to Apollo in the Langley hot-shot tunnel at Mach 20 in nitrogen [20]. However, the Reynolds number based on freestream conditions and model diameter was about 1×10^5, and the flow was apparently again all laminar. The flow is again attached along the windward meridian at 33-deg. AOA. At zero AOA, it separates on the afterbody at an arclength to model radius ratio of about 1.4.

Lee et al. measured heat transfer to Apollo in an arc-jet at Mach 13.8 [21]. The afterbody flow was separated at zero AOA, and attached on the windward side at 33-deg. AOA. The Reynolds numbers were only about 800 based on model diameter and freestream conditions, and the flow was apparently all laminar. The data is plotted against measurements from several other high-enthalpy facilities and all appear to provide laminar flow.

Lee et al. later measured afterbody heat transfer to Apollo in an arcjet at Mach 5.8 to 8.3 [22]. The model was 0.0065 scale and had a teflon nosecap to study ablation effects. The Reynolds numbers based on diameter were 200 to 22,000, so the flow was almost certainly laminar. Afterbody heat transfer decreased by a factor 2 with ablation.

Kemp measured afterbody pressures on Apollo in the helium tunnels at Ames, at Mach 10 to 21, and in air at Mach 14 [23]. The Reynolds numbers based on freestream conditions and model diameter ranged from $0.36 - 1.15 \times 10^6$ in helium and were 11,800 in air. Free-flying telemetered measurements were made to avoid sting-support interference. Although transition is not discussed, it appears that the data are all laminar.

Akin measured heat transfer to Apollo in a combustion-driven shock tunnel using both air and carbon dioxide [24]. The Reynolds numbers are not given, but the stagnation pressure was 285 atm. and the freestream velocity was 12 kft/s in CO_2 and 13 kft/s in air. There is no evidence of transition in the heat-transfer distributions on the blunt face, despite the substantial stagnation pressures. It would be interesting to see some further analysis to understand why transition apparently did not occur.

Gorowitz measured heat transfer to a 0.01875-scale Apollo model in the 12-inch shock tunnel at North American Aviation, at Mach numbers 15.5, 16.8, and 18.3 [25]. The AOA was zero to 40 deg. The geometry was from a preproposal stage and does not duplicate the final geometry. The full-scale diameter was 160.0 in., with a 192.0-in. blunt-face radius, a 35-deg. afterbody half-angle, and an 8.0-in. toroidal radius at the junction between the blunt face and afterbody. Pressure and heat-transfer data are tabulated at unit Reynolds numbers of $1.64 - 2.67 \times 10^5$/ft., depending on Mach number. Ten thin-film gauges were used on the model. Since the model diameter was 3.0 in., $Re_D = 0.41 - 0.67 \times 10^5$, and the data are probably all laminar. Here, Re_D is a Reynolds number based on freestream conditions and diameter; lacking sophisticated computations, this is often the only relevant Reynolds number that is readily available. Comparison data were also obtained on a 1.75-in.-dia. sphere.

Additional Ballistic-Range Data for Apollo

Following the completion of Ref. [17], additional ballistic-range data was located. Since this data had the potential to supply additional information regarding transition on Apollo, it is summarized here. However, so far all the data appear to be laminar.

DeRose measured lift, drag, and trim on Apollo capsules in the Ames ballistic range at high Mach numbers, including the use of the counterflow shock tunnel [26]. The report contains three shadowgraph images at $Re_D = 52,500 - -214,000$. DeRose made shots to $Re_D = 3.06 \times 10^5$ at Mach 11.2 (run 1512). If these shadowgraphs can be retrieved with good quality they might shed light on transition on the afterbody and in the wake. Unfortunately, no NASA-Ames photo numbers are given, so there is no known archive for such photos.

Sammonds measured forces and moments on Apollo capsules and slightly modified shapes, in the ballistic range at Ames at Mach numbers from 5 to 35 [27]. The counterflow shock-tunnel was also used. The Reynolds numbers based on freestream conditions were from 40,000 to 350,000. No effect of Reynolds number was observed in the force and moment data, suggesting it was all laminar. Thirteen shadowgraphs are included and these are said to show transition moving forward in the wake as the Reynolds number increases. However, the PDF images from STI are not good enough to see clearly. The original images might be helpful for understanding wake transition. The photos do not include any archival image numbers, and the small models were only 1 cm in diameter, limiting shadowgraph resolution.

Lawrence et al. measured forces and moments on Apollo capsules in Range G at AEDC [28]. The Mach numbers were 6 and 8.5, and $Re_D = 50,000 - -240,000$. The focus of the tests was on resolving anomalies in low-Reynolds number aerodynamics, between the AS-202 flight and previous ground tests. The data are probably all laminar, and there is no discussion of transition. Shadowgraphs were obtained but none are shown. It is not clear if any have been archived.

Isolated Roughness Effects on Apollo Transition

There are very few studies of the effect of isolated roughness on transition on hypersonic or supersonic blunt bodies. Public-release flight data for transition on blunt bodies is reviewed in Ref. [10]. Blunt bodies are difficult to study in ground experiments, since blunt models must be relatively small if they are not to unstart the wind tunnel. Few facilities can achieve sufficiently high Reynolds numbers to study transition on blunt bodies, and these tend to be expensive. Most of the DoD interest has been in uniformly ablating nosetips. Most studies of the effect of isolated roughness have been carried out for two purposes: (1) determining the local heating around isolated roughnesses, or (2) using rows of isolated roughnesses for tripping purposes. Thus, any transition data was usually obtained as a byproduct.

Effect of Protuberances on Apollo Heating Bertin 1966 and Emerson 1964

Bertin summarized the wind-tunnel data for protuberance and cavity effects on Apollo heating [29], as is also discussed in Ref. [9]. The smooth-wall data are also reviewed. However, there is no

explicit discussion of transition. With the computational methods available in 1966, it would have been nearly impossible for Bertin to distinguish interference heating and vortical-wake heating from heating induced by transition in the wake of the protuberances and cavities.

Bertin collects previously-reported data from the Ames and Langley tunnels. He also reports new data from the Mach-10 tunnel C at AEDC and from the 21-inch hypersonic tunnel at JPL. Bertin reports the use of a 0.045-scale Apollo model in Tunnel C for smooth-wall heat transfer, and a 0.090-scale model for heat-transfer near cavities and protuberances. The 0.045-scale data is reported in detail in Ref. [30] and appendices. The 0.090-scale data appears to be the same that is reported in 1069-page detail in Ref. [31]. The pretest report contains additional information on the Tunnel C experiment [32]. An 0.02-scale model was tested at JPL; the basic data are reported in Refs. [33] and [34].

Fig. 1 sketches the protuberances and cavities in the Apollo command module. Bertin states that the full-scale shear pads are 6.5-in. dia. and protrude 0.55 in. above the surface. The full-scale scimitar antenna is 2.1-in. wide and extends a maximum of 8.1 in. above the surface. The full-scale umbilical fairing protrudes 3.1-in. above the surface. The windward tower well is a cavity 14.8-in. long by 5.5-in. wide with a maximum depth of 4.6-in.

According to Ref. [31], the full set of blunt-face protuberances is larger than those shown in Bertin's approximation. Fig. 2 shows 3 compression pads plus 3 shear pads plus an oxidizer dump, whereas Fig. 1 shows only the 3 shear pads. Recall that the Tunnel C model was 9% scale. Some of the Tunnel C models shown in Ref. [31] also show blunt-face ramps leading to the umbilical fairing. The Tunnel C models were 0.02-in.-thick 310 stainless with 294 thermocouples welded on the inside. Note that the 9.0% model was 6.930 inches in radius (Fig. 2). Per the imperfectly-reproduced foldout drawing at the end of Ref. [32], the compression pads were centered 5.332 in. from the model center, with a diameter of 0.54 in. Two of the compression pads had a thickness of 0.045 in. and one was 0.099 in. The oxidizer dump was 0.445-in. dia., 0.009-in. thick, and located at a radius of 6.164 in. The shear pads are located at the same radial location as the compression pads; although some detail is shown on the fold-out drawing, it is difficult to read. However, the shear pads include some kind of 3D protrusion at a radius of 5.675 in. that protrudes 0.150 in. at a 37.85-deg. angle. Thus, there seem to be some unexplained contradictions between Bertin's summary and some of the details in the source reports. The protuberances were fastened to the model with number 2-64 screws. Emerson plots and tabulates over 1000 pages of heat-transfer data, from several different configurations.

Bertin notes that the laminar heating on the smooth configuration was essentially independent of flow conditions and test facility. Bertin compares the pressure measurements to Newtonian values, which is all he had available. The smooth-wall heating measurements were compared to Lees' well-known laminar theory [35]. The Tunnel C measurements were carried out at Reynolds numbers based on body diameter and freestream conditions varying from $Re_D = 0.2 \times 10^6$ to $Re_D = 1.2 \times 10^6$, and the JPL measurements were carried out at $Re_D = 0.17 \times 10^6$ to $Re_D = 0.62 \times 10^6$; both these values are fairly low. Ref. [31] gives the Tunnel C freestream Reynolds number range as 0.33 to 2.0 million per foot, with a 13.86-in.-dia. model. Bertin plots heating rates normalized by the value at the stagnation point at zero angle of attack. The smooth wall data appear to be laminar, since they agree fairly well with Lee's laminar theory.

Bertin presents the heating data as a ratio to the value measured on a smooth model at the same location, calling these 'interference heating factors'. Interference factors in the wake of shear pad 1 ranged from a typical 1.5 to as high as 2.7, possibly due to transition or possibly to vorticity in the wake. Since this pad was in a subsonic region the heat transfer was unaffected upstream of the pad.

Upstream of shear pads in the supersonic region, interference heating factors were as large as 8, probably due to shock/boundary-layer interactions. The effect of Reynolds number on the interference factors depended on the location studied, so Reynolds number effects cannot be easily used to infer transition. However, in the wake of shear pad 1, the interference factors consistently rose with Reynolds number. A detailed reanalysis would be necessary to establish a clear physical cause for this effect.

Bertin states that the height of shear pad 3 is about twice the momentum thickness in the incoming boundary layer [29, p. 13]. Thus, these protuberances are nontrivial.

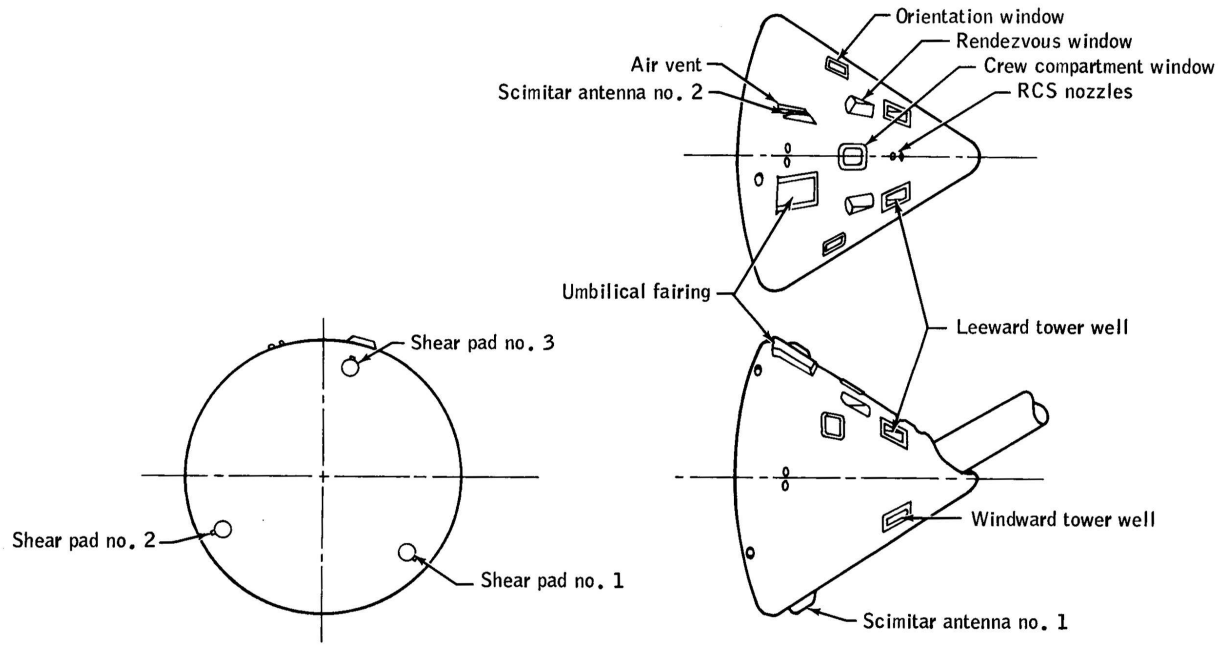

Figure 1: Sketch of the Apollo Command Module illustrating the cavities and protuberances. From Ref. [29, Fig. 2]

Effects of Apollo Surface Cavities and Protuberances on Heating – Jones 1965

Jones and Hunt measured heat-transfer to the Apollo command module in the Mach-8 tunnel at Langley, using phase-change paint [36]. Heating increases were measured near the shear pads, umbilical fairing, reaction control jets, and antenna, for $Re_D = 0.13 - 1.5 \times 10^6$. The models were 4.00-in. in diameter, the shear pads were 0.016 in. high, and the adjacent tension ties were 0.040-in. high. The heating increases were analyzed in terms of interference factors, as in Ref. [29]. If transition occurred in the wake of the roughness elements, there was no way for Jones et al. to distinguish it from vortex-induced heating, and there is no discussion of transition.

Hunt and Jones reported more measurements of a similar type, 3 years later [37]. It is again difficult to see if any of the roughnesses induced transition, for similar reasons. Fig. 26 in Ref. [37] appears to show transition on the afterbody as the Reynolds number is increased, but the authors do not believe it is due to transition since the rise begins at the same location independent of Reynolds number.

Jones and Hunt also summarized these measurements in Ref. [38]. However, this document does not appear to contain any additional information that is useful for the present purpose.

Catalog of Apollo Tripping Experiments

Apollo models used to obtain data with isolated tripping roughnesses are summarized in Ref. [39]. The entire Apollo wind tunnel program was summarized in Refs. [40] and [41]. Note well that Ref. [41] is a later version than Ref. [40] despite the erroneous date in the NASA STI citation for the latter.

Fifteen trip configurations were designed and tested; configurations 7 to 10 and 13 to 15 involve trips on the blunt spherical face, while the rest involve trips on the conical afterbody for launch studies. Configuration 7 is shown in Fig. 3. It appears that the stagnation point on the blunt face at the nominal angle of attack of about 33-deg. is expected near the upper center of the face, so the tripping spheres are located in a semi-circular arc downstream of this stagnation point. Configuration 7 was tested in AEDC Tunnel B, using model H-2, as documented in SID report 62-993, where SID is the North American Aviation Space and Information Division. Ref. [30] documents 7 runs with trip 7 at unit Reynolds numbers of 0.0833×10^6/in. and 0.30×10^6/in. and at angles of attack of 28 to 40 deg.

Configuration 8 was similar except the sphere diameter was increased from 0.694 in. dia. to 1.042 in. dia. (full scale) and the arc of trips was located

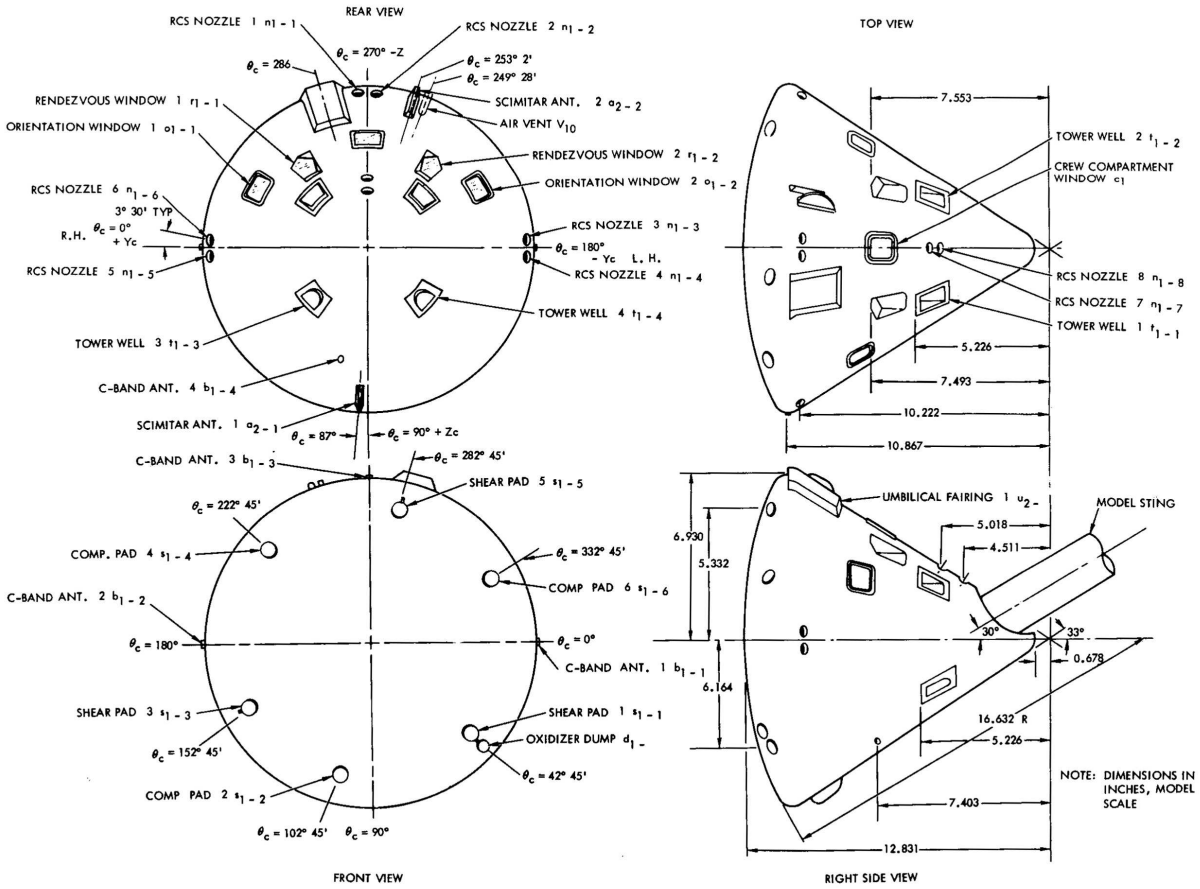

Figure 2: Sketch of the H-11 Heat Transfer Model of the Apollo Airframe 011 Command Module illustrating the cavities and protuberances. From Ref. [31, Fig. 1]

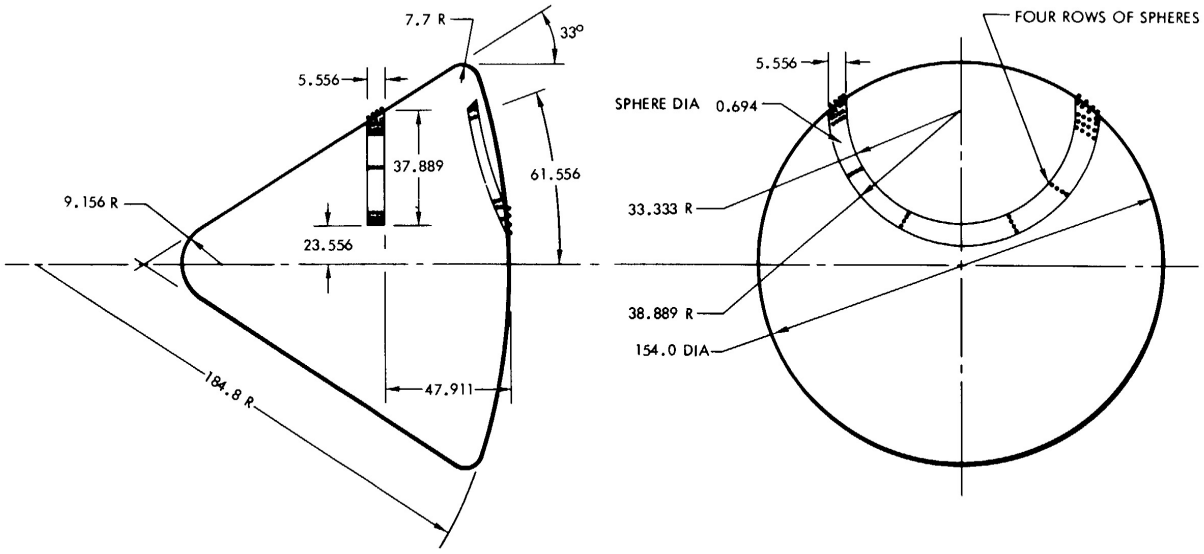

Figure 3: Sketch of the Apollo Command Module illustrating Boundary Layer Tripper No. 7. Full Scale Dimensions in Inches. From Ref. [39, Page 22-9]

farther from the stagnation point. It was also tested on model H-2 in Tunnel B, in 11 runs at zero AOA and units Reynolds numbers varying from 0.0364×10^6/in. to 0.295×10^6/in. [30].

Configuration 9 was similar to Configuration 7 except for the radii of the arc of trips. It was tested twice on model H-2 in Tunnel C as apparently reported in SID 62-993, SID 62-1214, and SID 63-688. Ref. [30] reports 8 runs at AOA ranging from 28 to 40 deg. and unit Reynolds numbers of 0.0833×10^6/in. and 0.200×10^6/in.

According to Ref. [30], *'Flow transition over the entry face of the command module was achieved, and its effect on the heat transfer distribution was shown. Flow transition on the afterbody of the command module was not attained.'* This data is to be discussed further below, although reanalysis will be required.

Configuration 10 changed to the use of grit trips, as shown in Fig. 4. Config. 10 was tested in the JPL hypersonic tunnel on model H-1 during test JPL 21-102 as apparently reported in SID 62-354 and SID 62-628. See the discussion of Refs. [33] and [34] (SID 62-628) below; the critical data from this test appear to lie in pages that are missing from the end of volume 2 of this report, and the search for pages A-1221 to A-1419 continues. SID 62-354 remains to be located.

Configuration 13 also uses a band of grit on the blunt face, and was tested in the Langley Unitary tunnel on model H-2 as reported in SID 62-1011 and SID 63-683. Per Garland Gouger of the NASA Langley library, the reference to SID 63-683 in Ref. [41] is a typo. Experiments with configuration 13 are not reported in the open literature.

Configuration 14, shown in Fig. 5, was tested on model H-2 in Tunnel C, as apparently reported in SID 62-1214 and SID 63-688. It uses four rows of staggered spheres in a similar arc band. There is a second band on the afterbody. Measurements on this configuration are not reported in the open literature either.

Configuration 15, shown in Fig. 6, was tested on model H-2 in Tunnel C, as reported in SID 63-1135 [42]. It uses spherical balls distributed uniformly over the blunt face, except near the centerline. Trip configurations 15 and another numbered 16 were tested in AEDC Tunnel C as reported in Ref. [42]. Trip configuration 15 was tested at freestream Reynolds numbers ranging from $0.083 - 0.166 \times 10^6$/in. and angles of attack ranging from 40 to 20 deg. The run summary shown in Table 5 of Ref. [42] does not show any runs with configuration 16, nor are any further details reported for this configuration. Figs. 6 and 7 in the Ref. include photographs of the trips, but the PDF's provided by NASA STI are unreadable. Ref. [43] contains plotted data for the tripped conditions on pp. A-776

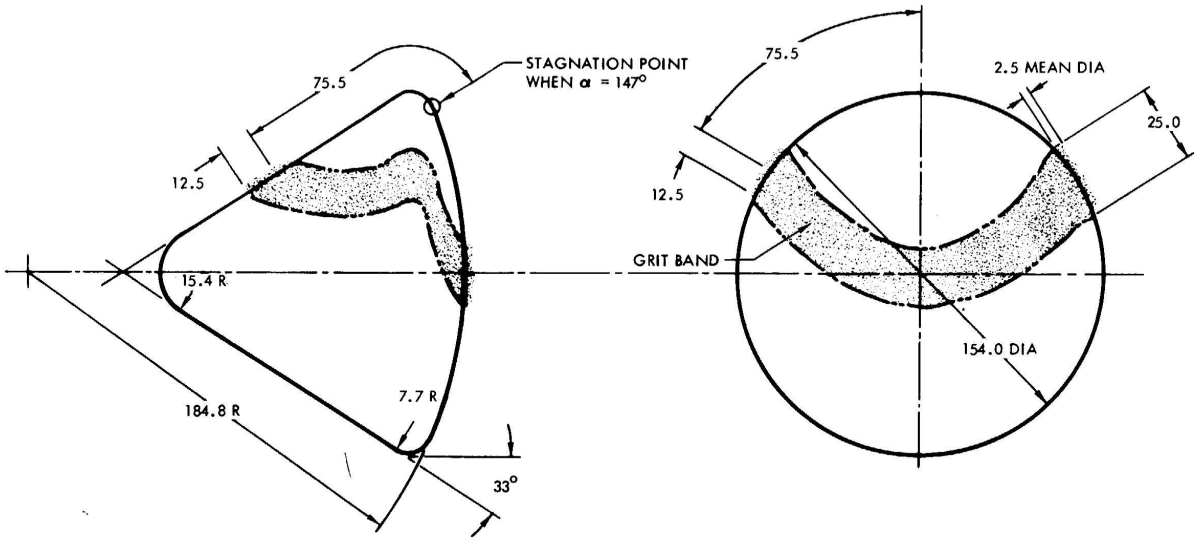

Figure 4: Sketch of the Apollo Command Module illustrating Boundary Layer Tripper No. 10. Full Scale Dimensions in Inches. From Ref. [39, Page 22-12]

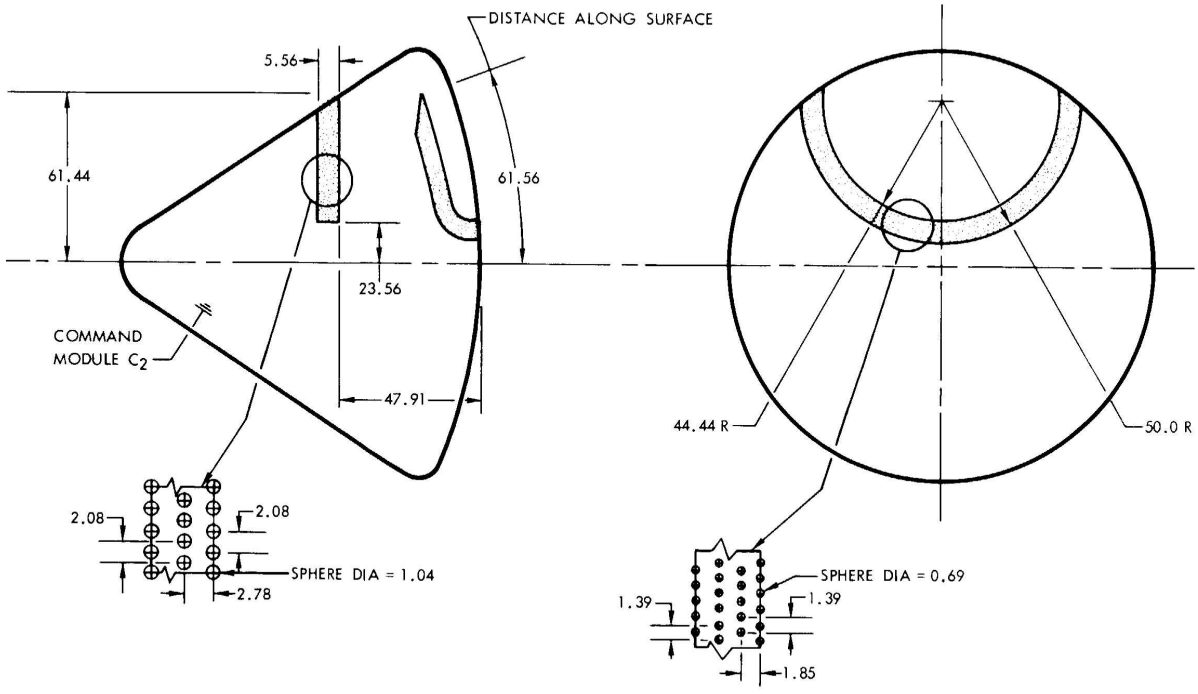

Figure 5: Sketch of the Apollo Command Module illustrating Boundary Layer Tripper No. 14. Full Scale Dimensions in Inches. From Ref. [39, Page 22-15]

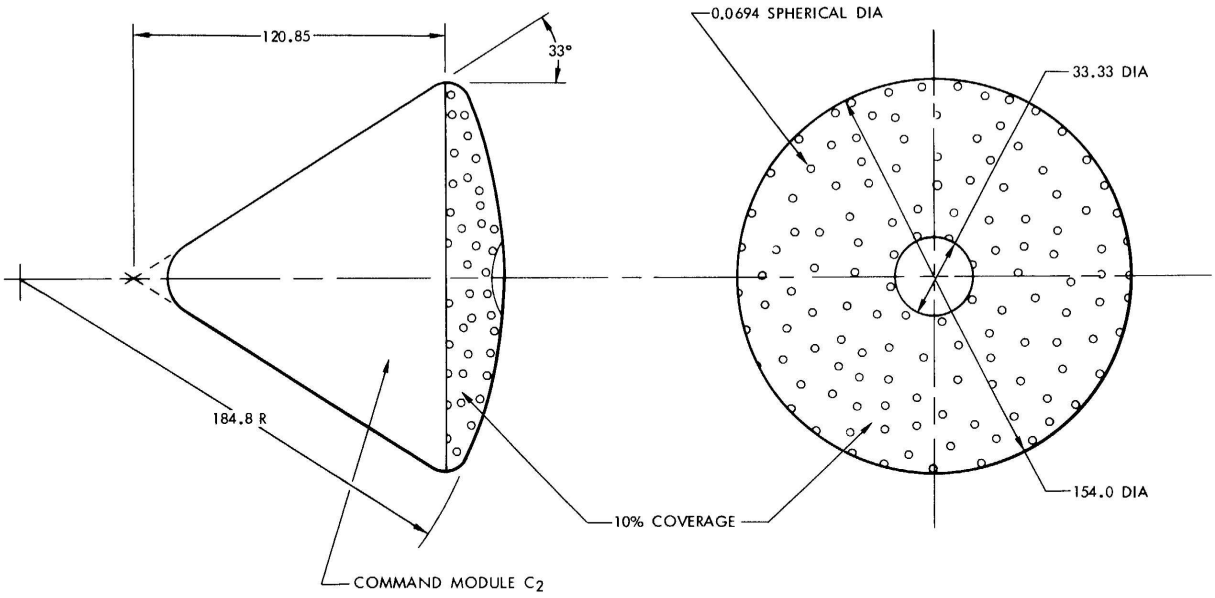

Figure 6: Sketch of the Apollo Command Module illustrating Boundary Layer Tripper No. 15. Full Scale Dimensions in Inches. From Ref. [39, Page 22-16]

to A-925. This large volume of plotted data would have to be reanalyzed to determine if transition was successfully tripped, and under what conditions and where. Ref. [44] contains tabulated data for these conditions, on pp. B-690 to B-789. The tabulated data are legible and could be typed into files, or possibly machine scanned.

Some of these studies contain data that shows the conditions under which these trips were effective in causing transition on the blunt face. These cases provide data for the effect of controlled roughness on transition under wind tunnel conditions. A reanalysis of this data appears warranted, but computations of the mean flow for a capsule at angle of attack are still not trivial.

Effect of Rows of Sphere Trips on Apollo – Biss 1962

As cataloged above, Biss measured tripped transition on the blunt face of Apollo in Tunnels B and C at AEDC [30]. The 0.045-scale models were instrumented with 98 thermocouples on the back of the 0.040-thickness stainless-steel skin. The plots are found on pp. A-182 to A-195 for the Tunnel B data and pp. A-636 to A-651 for the Tunnel C data [30, p. 10]. Biss states that *'It appears from the curves that boundary layer transition was achieved downstream of the trips on the entry face but not from the trips on the afterbody. The runs made at higher Re/in. in both tunnels showed a more pronounced variation . . . '* in heating. Per the run summary, the plotted Tunnel B data was all obtained with trip configuration 7, although both configurations 7 and 8 were used as part of AEDC configuration 31. The trip 8 data was obtained with the model off centerline. The plotted Tunnel C data were all obtained with trip configuration 9, which is again labeled AEDC configuration 31. Fig. 7 shows the configurations measured, along with some details on the runs carried out for each.

The Tunnel C data with AEDC configuration 31, trip 9, for groups 33 to 40 are plotted on pp. A-636 to A-651 of Ref. [45]. There were 4 runs at a unit Reynolds number of 0.0816×10^6/in. and four at 0.1999×10^6/in. Angle of attack ranged from 48 to 28 deg. The data would have to be reanalyzed to see what can be learned from them, and compared to the smooth-wall data. However, all the data appear to show tripping, so the onset of a tripping effect is not obviously present. The Tunnel C data for trip configuration 9 is tabulated on pp. B965 to B1003 of Ref. [46], groups 33 to 40. The unit Reynolds number is $0.0816 - 0.199 \times 10^6$/in. for AOA ranging from 28 to 48 deg., so these tabulated data appear to be the same data plotted in Ref. [45].

The Tunnel B data with trip configuration 7 in groups 79-82 are plotted on pp. A-182 to A-195 of Ref. [47] and tabulated on pp. B394 to B413 of

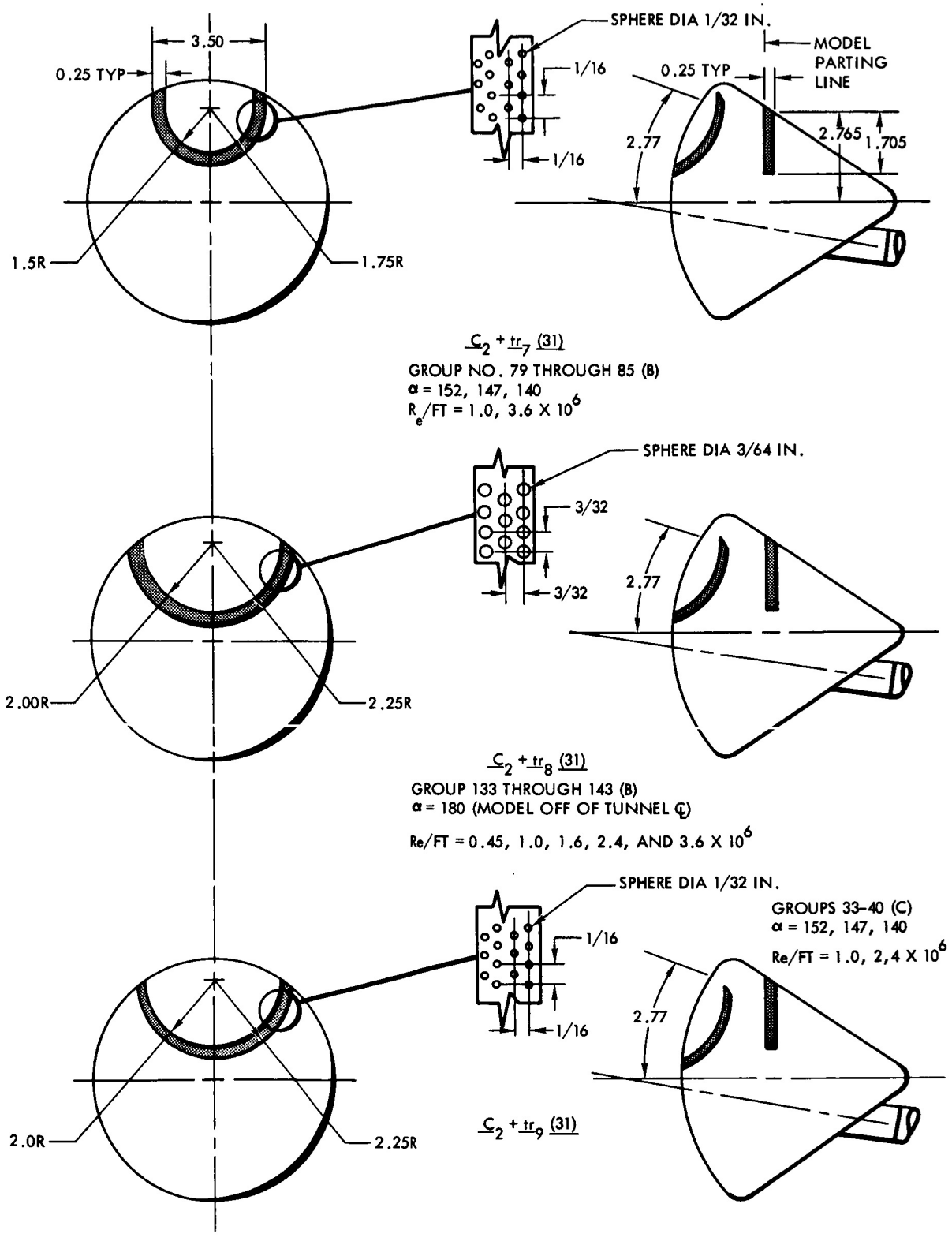

Figure 7: Boundary-Layer Trip Configurations for Tunnels B and C. From Ref. [30, Page 31]

Ref. [48]. The data were plotted for unit Reynolds numbers of 0.0808×10^6/in. and 0.2962×10^6/in., for AOA ranging from 28 to 40 deg. Most of the tabulated data appear legible. Comparing the plots for the high and low Reynolds numbers for the 33-deg. AOA case, pp. A-187 and A-193, some azimuthal rays appear to show the onset of transition with the increase in Reynolds number. For example, the 0-180-deg. line appears to show transition at $s/R \simeq -0.6$. However, the data need to be replotted and reanalyzed to determine if and where transition occurs.

The Tunnel B data with trip configuration 7 for groups 83 to 85 is tabulated on pp. B416 to B430 of Ref. [49]. The freestream unit Reynolds numbers are all 0.2962×10^6/in. and the AOA ranges from 28 to 40 deg. It appears that these tabulated data supplement and do not duplicate the plotted data, which will have to be digitized. The Tunnel B data with trip configuration 8 for groups 133 to 143 is tabulated on pp. B669 to B723 of Ref. [49]. The freestream unit Reynolds number ranges from $0.0364 - 0.294 \times 10^6$/in., in five steps, which may allow determining the Reynolds number variation. The angle of attack is zero for the data with trip 8, just as shown (with the opposite reference for AOA) in Fig. 7. This data would have to be analyzed with care to determine the thermocouples behind the arc of trips.

Distributed Roughness Effects on Apollo Transition

Effect of Grit Tripping Strip on Apollo – Fromm 1963

Refs. [33] and [34] describe tests of a 2.0% scale model of the smooth Apollo command module in the hypersonic wind tunnel at JPL. Fig. 8 shows the dimensions of the model and roughness. The full-scale dimensions were 154-in. diam., 184.8-in. radius of the spherical end, 7.7-in. corner radius, 33.0-deg. afterbody half-angle, and 15.4-in. afterbody vertex radius. A thin-skin model was used, with thermocouples welded on the inside. The model included five rows of thermocouples and a total of 44. The model diameter was 3.08 inches, and was tested at Mach numbers ranging from 6.0 to 9.0 and Reynolds numbers based on model diameter ranging from $0.06 - 0.8 \times 10^6$. Unfortunately, it appears that the model with the grit was only tested at Mach 6, 33-deg. angle of attack, and Re_D of 0.616×10^6 and 0.800×10^6. A shadowgraph was reported to show the effect of the transition grit, but the image is unreadable in the NASA STI PDF.

The data from the brief tripping study was obtained in Runs 88 and 89. The run conditions are described in vol. 1, but the actual heat-transfer data are not there, nor in volume 2, which ends at p. A-1220 while the table of contents lists A-1419 as the last page. The search for pages A-1221 to A-1419 continues. Unfortunately, neither JPL nor NASA STI nor the NASA Langley library seem to have copies, so these data may be lost.

Previous Reviews of Transition on Blunt Models

Transition on blunt nosetips was a major DoD concern through the 1970's. Well-known reviews of this case were developed by Batt and Legner [15, 50], and Reda [13]. The Passive Nosetip Technology (PANT) program was undertaken to understand the related issues; although many of these reports are still limited distribution, some are public release [51, 52, 53]. The roughness generated by laminar ablation is generally not much larger than the boundary-layer thickness; much larger roughness can also be generated by ablation, apparently only after the boundary-layer has become turbulent [54].

Excellent photographs of the laminar-ablated surface roughness of 24 typical nosetip materials were reported by Eitman and DeMichaels [55]. Example of these images are shown in Figs. 9 – 11. These images are for a sample nosetip made of FWPF (fine weave pierced fabric) PAN SR-25PA, billet 903-1-RZ1, with a 1.00-in. diam. nose, ablated in the AFFDL 50 MW arcjet at 76 atm. in the ramp mode, with peaked enthalpy. Ablation flattens out the nosetip geometry, as shown in Fig. 9.

The model is then sectioned, vacuum mounted in thermosetting plastic, and polished. Fig. 10 shows a cross-section. The vertical Z yarns of the woven carbon-carbon can be clearly seen; these ablate at a faster rate than the matrix and transverse yarns, causing a characteristic pattern in the surface roughness. The scale of the image is shown in the lower right of Figs. 10 and 11; the vertical Z yarns are roughly 1.3 mm apart.

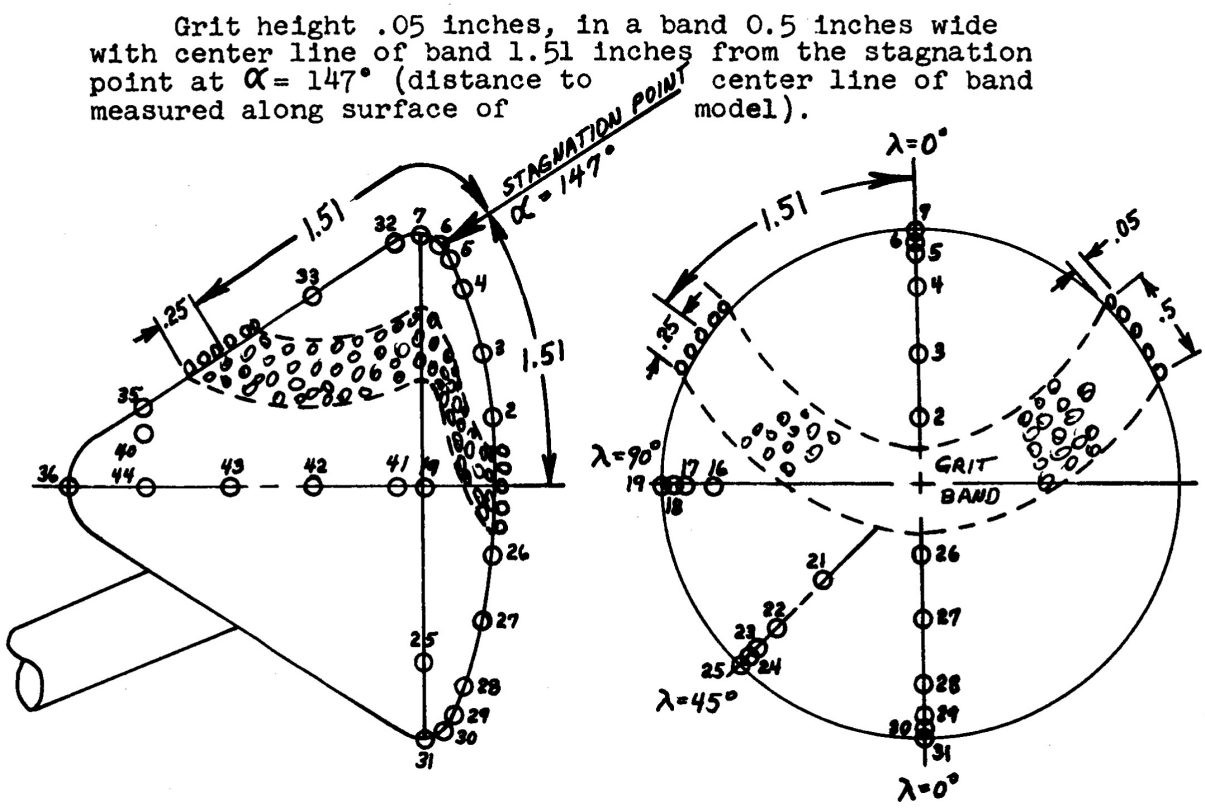

Figure 8: Sketch of the Apollo Command Module with Transition Grit. Model TR10. Model Scale, Dimensions in Inches. From Ref. [33, Page 8]

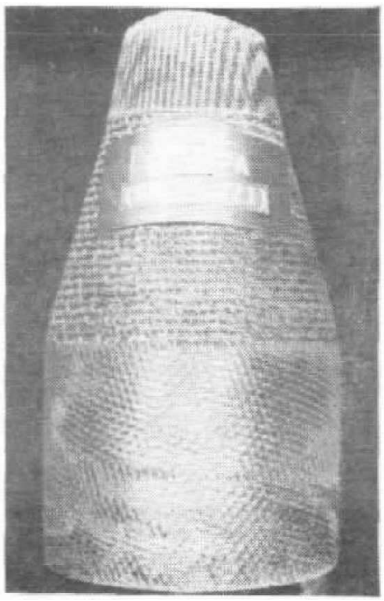

Figure 9: Side View of Laminar-Ablated FWPF Nosetip. From Ref. [55, Fig. 77]

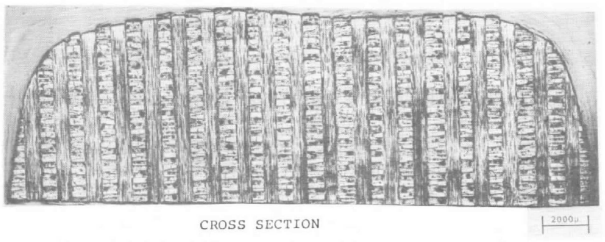

Figure 10: Cross-Section of Laminar-Ablated FWPF Nosetip. From Ref. [55, Fig. 77]

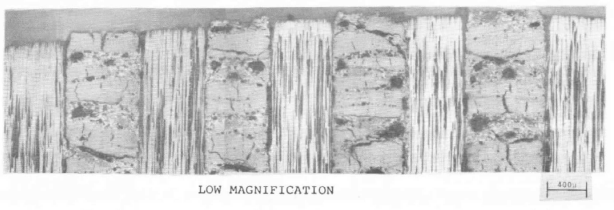

Figure 11: Low-Magnification Image of Laminar-Ablated FWPF Nosetip. From Ref. [55, Fig. 77]

Under low magnification in Fig. 11, the surface roughness can be seen more clearly. Microroughness measurements were made on the Z yarns (mean of 0.98 mil), the transverse yarns (0.18 mil), and the matrix pockets (0.42 mil). The peak microroughness height for this material was of the order of 1.5 mil [55, Fig. 35]. The median macroroughness height was 3.0 mil [55, Table 6]; this value considers the regular pattern of peaks and valleys corresponding to differential ablation between the yarns and the matrix. The peak macroroughness height was of the order of 6-8 mils [55, Fig. 56]. Eitman and DeMichaels also measured the porosity and other properties of these composites; as is evident from their discussion, it is not certain which characteristics of the roughness have the largest effect on nosetip transition in flight. The largest roughness in a surface usually causes the earliest transition downstream, but an average roughness is usually used to characterize the roughness of nosetip materials.

The 'blunt body paradox' refers to the paradoxical early onset of transition on nominally smooth blunt bodies, for which the favorable nose-region pressure gradient and low wall temperatures were expected to produce laminar flow. It appears that Morkovin coined the term [56, 57]. Stetson provided the most recent review of this topic [58]. See the discussion of the related public-release flight data in Ref. [10]. The Mark-2 [59] and X-17 [60, 61] datasets are the most well known. Most of the flight data for these vehicles are still classified or limited.

Wisniewski reviewed highly cooled blunt bodies in 1960 [62]. He correlated transition using a Reynolds number based on displacement thickness and the ratio of wall to total enthalpy. Although he notes that *'... cooling may cause the boundary layer to go from laminar to turbulent flow,'* he does not evaluate roughness effects, which the present author believes is the most likely mechanism for this effect. Nevertheless his discussion and list of references is useful.

Potter and Whitfield wrote a brief discussion of the effects of cooling and roughness in 1961 [63]. They show that surface roughness in previous experiments could explain the reversal of the movement of transition with wall temperature, if a (proposed) different correlation is used. This shows the importance of treating a wide variety of data with a systematic comparison of correlations, which of course takes a substantial effort.

Abbett et al. reviewed the literature for the PANT program in 1975 [52]. Smooth-wall blunt-body transition was of particular interest, and the

flight data for the Mark 2, X-17, and NACA programs were discussed. The PANT correlation was generalized for blowing due to ablation [51].

Finson wrote another review in 1976-78 [64, 65]. Finson believed that Re_k correlated the data better than k/θ, and preferred to include a curvature term. He provides a good summary of the limitations of the available data and the difficulties in using any of the correlations.

Ground-Test Experiments for Transition on Other Blunt Models

Although ground-test data for supersonic and hypersonic transition on very blunt models is relatively scarce, considerable data does exist. The following summarizes the public-release literature in this area, in chronological order.

Cones and Hemispheres at Mach 4 and 8 in the Ballistic Range – Seiff 1957

Seiff et al. measured transition on blunt cones, hemispheres, and spheres, in the Ames ballistic range at Mach 4 and Mach 8 [66]. The Mach-4 experiments should have low noise, but the Mach-8 experiments used a counter-flow wind tunnel, and therefore suffered from visible levels of noise in the shadowgraphs. The basic model was a 60-deg. included-angle blunt cone, with a base radius of 0.863 in. and a nose radius of 1/3 the base radius. Measurements were also made on a 60-deg. included-angle sharp cone, a hemisphere with a 0.863-in. base radius, and a 3/8-in. dia. sphere. Three levels of surface finish were used, and characterized with interferograms. Transition was inferred from spark shadowgraphs.

For the blunt cones with the least polish, at Mach 8.3, and $Re_D = 4.8 \times 10^6$, transition was often asymmetric, with the turbulent side remaining the same regardless of whether it was windward or leeward. This was taken as due to the variability in surface roughness. The highest polish did not increase the amount of laminar flow, perhaps because it was still too rough.

The sharp cones were laminar to an arc-length Reynolds number of 6.7×10^6, at Mach 8.3, with a similar finish. Seiff et al. concluded that bluntness increased the sensitivity of transition to surface roughness. The hemispheres with the coarsest finish appeared to become turbulent at Mach 8 at an arclength Reynolds number of 20,000. At the low-noise Mach 4 condition, transition began at an arclength Reynolds number of less than 800,000. Since the hemisphere shadowgraphs were difficult to interpret, the results are uncertain.

Seiff et al. analyzed the roughness height at the stagnation point and determined it to be roughly 1% of the boundary layer thickness, which was thought to be sufficient to have a substantial effect on transition. It would be very good if the original shadowgraphs could be recovered for reanalysis. However, it appears that nearly all the shadowgraphs from the Ames range have been lost, except for those which are numbered in the reports and were therefore saved in the Ames photo archive (see the discussion in Ref. [9]).

These results are worthy of further analysis, although many of the details have been lost. Further ballistic-range experiments of this type should be considered, since they can have the advantage of being free of tunnel-wall radiated noise, when the counterflow is absent.

Two-inch Hemispheres at Mach 5 – Cooper 1959

Cooper et al. measured transition on two-inch hemispheres in a Mach-5 open-jet wind tunnel at Langley, for unit Reynolds numbers as high as 77.4×10^6/ft [67]. The hemispheres were polished to 10-20 microinches, but the polish degraded under the pitting action of impinging particulate. Although the pits were polished between runs, the original surface finish could not be maintained. However, data was carefully taken almost immediately after the model was introduced into the flow. The thin-skin models were instrumented with 6-8 backside thermocouples. The original smooth models were laminar to Reynolds numbers based on diameter and freestream conditions of $Re_D = 12.1 - 12.9 \times 10^6$, or freestream unit Reynolds numbers of $72.6 - 77.4 \times 10^6$/ft. After the test the model contained pits about 0.002 to 0.003 inches in diameter. When these pitted models were tested without repolishing, transition occurred at $s/R = 0.35$, where s is the arclength from the stagnation point and R is the radius of the sphere. The ratio of wall temperature to stagnation temperature was typically 0.53 to 0.66.

This test shows that very high transition Reynolds numbers can be obtained on blunt models if the surfaces are highly polished. It also shows the sensitivity to small roughness. Both these remarks are in agreement with flight data [10]. Unfortunately, the pitted roughness properties were not measured, so the test does not provide any data relating roughness height to transition location.

19-inch Hemispheres at Mach 2.48 to 3.55
Bandettini 1959

Bandettini et al. measured transition on 19.02-inch-dia. hemispheres in the 8 by 7-ft. Unitary-Plan supersonic tunnel at Ames [68]. The initial surface roughnesses were 50, 580, and 2760 microinches, and unit Reynolds numbers ranged from $0.96 - 4.78 \times 10^6$/ft. Tunnel freestream particulate caused pits on the 50-microinch hemisphere, ranging in depth from 1500 to 2500 microinches. Transition was determined from shadowgraphs or thin-skin thermocouples. Most of the data were obtained at Mach 3.07. Before the appearance of these pits, the smooth hemisphere was laminar to 90-deg. from the stagnation point (the last station), to $Re_D = 7.57 \times 10^6$ and $Re_\theta = 660$. At these high Reynolds numbers, the pitted smooth model or the rougher models showed transition at about 50-deg. from the stagnation point. A page of tabulated data is presented to show the location of transition for the various rough models at various unit Reynolds numbers, and a good description is given for the model roughness and how it was characterized. The data appear worthy of reanalysis with modern approaches.

Two-inch Cold Hemispheres at Mach 5
Cooper 1960

Cooper et al. later measured transition on two-inch cooled hemispheres at Mach 5 and a freestream Reynolds number of 73.2×10^6/ft [69]. The stagnation temperature was about $400°F$ and the initial ratio of wall temperature to freestream stagnation temperature varied from 0.16 to 0.65. Thin-skin models with backface thermocouples were used to infer transition. The initial wall temperature was either $100°F$ (room temperature) or $-320°F$ (liquid nitrogen). The model roughness was 2-3 microinches rms with isolated scratches and pits with depth about 10-20 microinches.

The test with the hot wall was in essential agreement with the earlier measurements [67]. Transition on the hot model *'...resulted from surface roughness caused by the impact on the model surface of small particles in the airstream.'* Pits of 0.005 in. dia. were commonly observed under a 40-power microscope. The rim of the pits was probably surrounded by a raised edge, and raised edge heights of 1/10 of the diameter were suggested as a reasonable possibility. *'During two of the four cold tests, the boundary-layer flow changed from turbulent to laminar over large regions of the hemisphere as the model heated.'* Cooper et al. did not believe this was a roughness-related effect, based on simple Re_k estimates, but the present author believes this data could be analyzed as a roughness-induced effect, similar to the one observed by Stetson [70, 11]. As the model heats up, the boundary layer thickens, and the relative height of the roughness decreases.

Sphere-Ellipsoids at Mach 3 – Deveikis 1961

Deveikis et al. measured transition on roughened sphere-ellipsoids at Mach 3 in the Langley 9 by 6-foot thermal structures tunnel, at $Re_D = 2.76 \times 10^6$ and $Re_D = 4.25 \times 10^6$ [71]. The radome-like models had a nose radius of 2.25 inches and were tested with surface roughnesses of 5, 100, and 200 microinches. The thin-skin models were instrumented with backface thermocouples, which were used to infer transition location.

Transition onset locations varied from $s/D = 0.1 - 0.5$, where s is the arclength from the stagnation point and D is the model diameter. The surface finish on the 5 microinch model degraded by 'only' 20 microinches after the test, since efforts had been taken to reduce airstream contamination. With the 5 and 100 microinch models, data was only obtained at the higher Reynolds number, due to instrumentation breakdowns. Transition was promoted by surface roughness and boundary-layer cooling. Transition on the rough models was delayed when they were heated. These measurements should be recomputed with modern methods to compare them to various correlations.

Blunt Noses at Mach 2.2 – Jackson 1961

Jackson et al. measured transition on six axisymmetric bodies at Mach 2.2 in the four-foot supersonic tunnel at Langley [72]. The thin-skin heat-transfer models had 12-in. base diameters and were tested at zero AOA and adiabatic-wall conditions. Freestream unit Reynolds numbers ranged from $1.4 - 6.5 \times 10^6$/ft. Carborundum grit of 0.039 in. was used on most models to induce transition; this grit was said to be higher than the boundary-layer thickness, but was used due to the difficulty of tripping these flows. The smooth hemisphere remained laminar to the maximum Reynolds number, and a local $Re_\theta \simeq 700$. For the hemisphere with grit, the model was laminar for $Re < 2.7 \times 10^6$/ft. At $Re = 3.4 \times 10^6$/ft., the boundary-layer began to be transitional just downstream of the roughness. However, the hemisphere with grit never became fully turbulent, even at the highest Reynolds number.

A smooth hemisphere-cone model was laminar to the maximum Reynolds number. This model had

a 4-in. nose radius and a 14.5-deg. half-angle. However, when a strip of 0.025 to 0.028-in. grit was applied on the model face, the flow was transitional for the lower pressures and fully turbulent only for the higher pressures. To make the flow fully turbulent at the lower pressures, a second grit strip was applied in the region of adverse pressure gradient.

Model C had a blunted face; the geometry is not specified. The smooth-wall model C transitioned behind the shoulder at the maximum Reynolds number. Just as with the sphere-cone, a first roughness strip only tripped the flow at the higher Reynolds number, and a second strip had to be added in the region of neutral to adverse pressure gradient to trip at the lower Reynolds number. Models D and E had different levels of blunting and similar performance.

These data appear useful for comparing to various roughness-induced transition correlations. Although the Mach number is low, the blunt-body flow may be only weakly dependent on Mach number. The non-spherical shapes shed some light on the effect of variations in pressure gradient, but the geometries would probably have to be digitized from the drawings.

Hemisphere-Cylinders at Mach 10.4 and 11.4
Dunavant 1967

Dunavant et al. measured transition on hemisphere-cylinders with a 6-in. diameter at unit Reynolds numbers of $0.23 - 2.2 \times 10^6$/ft [73]. Four surface finishes were tested: a 4-microinch smooth surface, two surfaces with hemisphere-like close-packed roughness arrays with heights of 0.025 and 0.050 in., and a random nodular roughened surface with an average height of 0.004 in. The latter was produced by spraying on molten copper. The measurements were made in the Langley 31-inch hypersonic tunnel, during the original continuous-flow operation, in the Mach-10 and Mach-11 nozzles. Transition was inferred from backface thermocouples on the thin-skin Inconel models. Although the study was focused on roughness-induced augmentation of stagnation-point heating, transition onset was apparently induced on the three roughest models at $s/D \simeq 0.2$ for $Re_D \simeq 0.3 - 1.0 \times 10^6$. The data appear worthy of reanalysis. Re_θ at transition onset was said to be 25-55 on these very rough models. No correlation of roughness-induced transition was attempted, although these data were among those included in Batt's PANT-based correlation [15].

Hemispheres at Mach 2.01 – Van Driest 1967

Van Driest et al. measured transition on 6.5-in.-dia. hemispheres in the JPL 20-in. supersonic tunnel at Mach 2.01 [74, 75]. Single rows of tripping spheres were placed on the hemisphere at various angles from 12.5 to 60 deg. from the stagnation point. Spheres with diameters from 0.004 to 0.015 in. were used. Transition was determined by sublimation of azobenzene. The sudden widening of the vortex path behind the trips was taken as the onset of transition. Unfortunately, neither the journal paper nor the AFOSR report give any detailed tabulations or plots of the fundamental data. Previously, Van Driest correlated roughness-induced on cones using $Re_{\delta^\star}/(1+0.5(\gamma-1)M_e^2)$ vs. $k/\delta^\star$. However, this gave a poor correlation to the new data on the hemispheres. Van Driest et al. therefore added a curvature term, and obtained a curve fit to $Re_{\delta^\star}/(1+0.5(\gamma-1)M_e^2)$ vs. $(k/\delta^\star)/(1+700(k/D))$. The cubic curve fit is given in the paper, and Van Driest argues that all the data therefore follow essentially the same law. This data would be very valuable if sufficient detail can be found to be able to reanalyze it; this seems doubtful at present..

Hemispheres at Mach 5 – Varwig 1970

Varwig measured transition on a hemisphere with roughness in a Mach-5 shock tunnel at the Aerospace Corp. [76] (see also Ref. [77]). Transition was inferred from heat transfer measurements with thin-film gauges placed between the roughness elements, with the equivalent surface heat transfer inferred from other turbulent boundary-layer studies. Roughness was applied to the 4-inch hemisphere using glass beads. The smooth-wall hemisphere was laminar to a maximum Reynolds number of $Re_D = 2.9 \times 10^6$, at the stagnation temperature of about 900K. For the 0.004-in.-dia. beads, transition onset moved from 20 to 15 to 10 deg. from the stagnation point as Re_D increased from 1.3 to 1.4 to 2.7 million. Although the rough-wall heat-transfer data is problematic due to the measurements at the base of the cavity between roughness elements, the transition data may be worthy of reanalysis. Varwig also compares to measurements on a 7-in.-dia. sphere by DiCristina in the Mach-5 tunnel at NOL – these data remain to be located.

Blunt Cones and Hemisphere at Mach 4
Coats 1973

Coats measured transition on a sphere-cone, hemisphere, and compound sphere, at Mach 4 and 8 [78]. The sphere-cone had a 1.466-in. nose radius and a 10-deg. half-angle. The hemisphere had a 2.932-in. radius, and the compound sphere had a 3.826-in. radius near the stagnation point. Transition was inferred from surface temperature gauges.

The useful data was obtained at Mach 4 in Tunnel A, as the instrumentation did not work well in Tunnel B at Mach 8. Unfortunately, it appears that transition always occurred on the axial cylinders that followed the blunt forebodies, so there is no data for transition on the blunt noses themselves.

Blunt Cones – Jackson 1974

Jackson measured transition on blunt bodies in NOL Tunnel 8 as part of the PANT program [53]. Four of the models were sphere-cones with nose radii of 0.75, 1.5, 2.5, and 3.5 inches and 8-deg. half-angles. A biconic and a laminar-ablated shape were also tested. All the models were grit-blasted to a surface roughness of 0.0035 inches. The experiments were carried out at Mach 5 and unit Reynolds numbers ranging from 0.42 to 7.4 million per foot. Backface thermocouples were used on thin-skin models to infer heat transfer.

The noise in the tunnel freestream noise was measured under different conditions. The RMS pressure fluctuations divided by the freestream dynamic pressure ranged from near 0.003 at the lowest Reynolds number to near 0.0007 at the highest Reynolds number. Detailed plots of the heat-transfer coefficient vs. arclength are shown for all runs. Transition moves forward as the unit Reynolds number and nose radius increases, but does not scale only with the nose-radius Reynolds number, perhaps because all models had the same surface roughness. The results are well documented and appear to be useful for evaluating transition-estimation methods.

Viking Aeroshell at Mach 8 – Creel 1974

Creel measured heating to the blunt sphere-cone Viking aeroshell in the NASA Langley Variable Density Tunnel at Mach 8 [79]. The model included isolated protuberances and cavities expected to be characteristic of the flight vehicle. Aeroheating was measured using fusible temperature paint. The model was 11.68 cm. in diameter, and was tested at freestream unit Reynolds numbers of $3.7 - 17 \times 10^6$/m. Interference heating was measured aft of the isolated surface flaws. Since there was no marked dependence of the nondimensional heating on the Reynolds number, it may be that all the measurements reflect interference heating that is basically laminar. This is not too surprising, since $Re_D < 2 \times 10^6$. A reanalysis of the protuberance wakes would be of interest.

Hemisphere at Mach 6 – Laderman 1977

Laderman measured transition on 14-in.-dia. porous and roughened hemispheres in Tunnel B at $Re_D = 2.8 - 6.2 \times 10^6$ [80]. Pitot tubes and hot-wires were used to obtain profiles of the flow at 40 deg. from the stagnation point. Four roughness overlays were tested: these had 'effective' peak-to-valley roughness heights of 1.44, 1.70, 2.36, and 4.77 mils. The model was internally cooled with liquid nitrogen. The flow was completely laminar with the smallest roughness under adiabatic conditions. Transition compared favorably to the PANT correlation. See also Ref. [81] for similar data with blowing effects from a porous hemisphere. These data should be reanalyzed with modern computational methods, but the details are available only in reports with limited distribution.

Blunt Bi-Cones at Mach 15-20 – Richards 1977

Richards et al. measured transition on blunt bicones in the VKI hot-shot tunnel at Mach 15-20 [82]. The Reynolds numbers based on freestream conditions and model base diameter were $1.2 - 5 \times 10^6$. The model nose radius was 0.75 in. and the base diameter was 7.00 in. The forecone had a 50-deg. half-angle followed by an 8-deg. half-angle aftcone. Transition was inferred from flush calorimeters. Transition Reynolds numbers based on momentum thickness Re_θ ranged from 250-400 on smooth models, and decreased 25% when 4-mil evenly distributed roughness was added. Unfortunately, the data is fairly sparse and not presented in much detail, so unless a more detailed report can be found a reanalysis does not appear to be warranted.

Hemispheres in the Ballistic-Range – Reda 1979

Reda and colleagues made several measurements of transition on various nosetip materials using hemispheres in the ballistic range. See, for example, Refs. [83] and [84]. Ref. [84] compares the performance of ATJ-S, CMT, Graphnol, 223 C/C, and FWPF materials. All flights were carried out at 16.0 kft/sec into air at $540°R$. The surface microroughness of the laminar pre-ablated specimens was measured using microscopy. The peak-to-valley heights for the bulk graphites varied from 0.168 mils for Graphnol to 0.383 mils for CMT to 0.638 mils for ATJ-S. The peak-to-valley heights for the woven materials were 0.422 mils for 223 C/C and 0.271 mils for FWPF. Nose radii varied from 0.4 to 1.25 inches. Transition was detected using electro-optical pyrometry images.

The smoother materials exhibit transition farther downstream or at higher Reynolds numbers, as shown in Fig. 12. Here, S is the arclength along the hemisphere from the nose, and R_N is the nose radius.

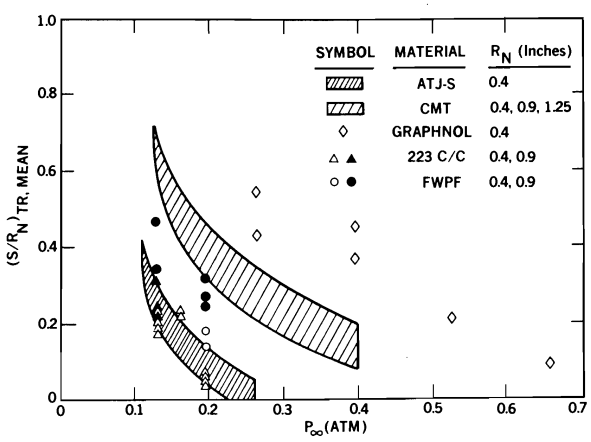

Figure 12: Transition Front Location vs. Freestream Static Pressure for Ballistic Range Measurements on Hemispheres. From Ref. [84, Fig. 8]

Correlations of this data are shown in Ref. [13]. The best fit was achieved with a correlation based on the roughness Reynolds number, Re_k.

Hemispheres with Small Craters at Mach 5
Todisco 1981

Todisco et al. measured transition on hemispherical nosetips in Tunnel 8 at NSWC including small craters that simulated the effect of particle impacts [85]. The nosetip radii were 2.5 and 1.0 inches, and the wall to stagnation-temperature ratio was 0.3. Unit Reynolds numbers varied from $1 - 20 \times 10^6$/ft., and transition was inferred from 75 backface thermocouples. The models were polished to 2-4 microinches and then the craters were machined using custom toolbits. Both single and multiple craters were tested.

At low Reynolds numbers the boundary layer remained laminar behind the crater. At higher Reynolds numbers, the boundary layer appeared to trip behind the crater but then relaminarized downstream; this behavior was termed 'crater transition'. At yet higher Reynolds numbers the boundary layer tripped and remained turbulent. For conical craters of depth $k = 0.020$ in., Re_k varied from about 1000 to 8000 for single-crater tripping, with the value and the variation in the value both increasing with the angle from the stagnation point. Todisco et al. note that the values are larger than those predicted using Van Driest and Blumer's correlation [74]. Craters with greater diameter-to-depth ratio were tripped at Re_k values that were 2-3 times lower than smaller craters. Deeper craters tripped at larger Re_k, in accordance with Van Driest's correlation, which attributes the effect to variations in k/R_N, where R_N is the nose radius. The PANT correlation is also used for comparison. Since the basic data are not given, reanalysis is not possible with public-domain information.

This report provides useful data. However, it would be better to have more details on how the experiments were conducted, so other correlations can be compared using modern computational techniques.

Hemispheres in the Ballistic Range – Wassel 1984

Wassel et al. measured transition on simulated nosetips using the rails in Track G at AEDC [86]. The models were made from tungsten, ATJ-S, 994-2 graphite, 223 carbon-carbon, and FWPF. The tungsten models were built with nose radii of 0.25 and 0.40 in. and surface roughness ranging from 1.7 mils to less than 10 microinches. The graphitic models had 3/8-in. nose radii and were preablated laminar in a plasma arc. Optical pyrometry was used to image the transition front in flight. Wassel's table 1 lists 11 shots at speeds all near 16 kft/sec, static range temperatures near $540°R$, and static range pressures ranging from 70 to 570 torr.

The smooth tungsten hemisphere was laminar at a range pressure of 570 torr and $Re_D = 2.9 \times 10^6$. The heating rate at the stagnation point was about 17×10^7 W/m^2. Wassel's results for transition location were not in good agreement with the usual nosetip-roughness correlations, for reasons that are not clear to this author. The PANT correlations given by Wassel include corrections for surface blowing effects.

Spheres at Mach 5 – Schöler 1990

Schöler measured boundary-layer transition on the front portion of spheres that were sting-mounted in the Mach-5 Ludwieg tube in Göttingen [87]. Transition was measured using liquid crystals. The brief summary paper shows laminar flow at $Re_D = 2 \times 10^6$, turbulent wedges behind roughness at $3 - 3.6 \times 10^6$, mostly turbulent flow at 4×10^6, and fully turbulent flow at 4.5×10^6. The roughness due to the liquid crystals is given as 0.01 to 0.02 mm, but the sphere diameter is not given in this brief summary report. The data might be very useful for reanalysis if more detail can be obtained, but none has so far been located.

Hemisphere at Mach 12 to 16 – Holden 1985-1992

Holden et al. have made many measurements of aeroheating and transition in the large shock tunnels

at CUBRC in Buffalo, NY. Many papers and reports have been published, but it can still be difficult to find specific details for configurations of interest.

Ref. [88] is primarily concerned with augmented turbulent heating at the stagnation point of blunt bodies. However, it also reports shock tunnel measurements on hemispheres with a 12-in. diameter. Fig. 9 in the reference shows transition onset at about 3 inches from the stagnation point for a freestream Reynolds number of 11 million per foot at Mach 11. Unfortunately, the temperatures are not given. For the same hemisphere at the same Mach number at a Reynolds number of 4 million per foot, the flow is completely laminar. Trip rings of 0.010 and 0.020 in. height were also used at different locations. However, the data is not complete enough to permit reanalysis.

Ref. [89] is primarily concerned with shock/shock interactions near blunt noses, but includes measurements of smooth and transpiration-cooled hemispheres in the Calspan 48-inch shock tunnel. Heat-transfer measurements were made with thin-film gauges. Freestream unit Reynolds numbers ranged from 4×10^4/ft. to 1.6×10^6/ft. and the large models had a 6-inch nose radius, leading to $Re_D \simeq 0.04 - 1.6 \times 10^6$, even at the high freestream Mach numbers of 12 to 16. Holden's fig. 14 shows that the smooth hemispheres were laminar to 4.3×10^5/ft. at Mach 16.2. Holden's fig. 16 shows an increase in heating on the rough transpiration-cooled hemispheres at about 40-deg. from the stagnation point, at both 3.2×10^5/ft. and 1.5×10^6/ft., with the coolant-flow off. Unfortunately, there is no clear data for transition (as opposed to slot-disturbance augmented laminar heating), and the roughness of the slotted transpiration-cooled nose is not clear. Ref. [89] is suggestive of the capabilities of the Calspan facilities, but in itself does not seem to contain useful data for comparison to improved methods of estimating transition.

Transition on Blunt Sphere-Cones at Mach 9
Zanchetta 1995

Zanchetta and Hillier measured transition on a blunt sphere-cone with a 5-deg. half-angle in the Imperial College gun tunnel at Mach 9 [90]. Thin-film heat-transfer gauges were used to infer transition. Zanchetta observed that for small nose-radius Reynolds numbers of 3×10^5 or less, increased nose radii delayed transition on the cone. For larger nose-radius Reynolds numbers, transition became sensitive to small surface imperfections, and small roughness elements in the subsonic region on the nose caused transition to jump forward to the sphere-cone junction. These observations are similar to those reported by Stetson [70], who suggested a different scaling; see also the discussion in Ref. [11]. However, few details are presented in this short conference paper.

More detail is available in Zanchetta's Ph.D. thesis [91]. Twelve nose radii ranging were tested at three unit Reynolds numbers. The nose radii varied from sharp to 25 mm, and the freestream Reynolds number was 7.5, 12.6, or 47.4 million per meter, with stagnation temperatures near 1100K. The diameter of the Mach-9 core flow is about 280 mm and the duration of steady flow is about 4-7 ms. In most cases it was still difficult to determine the locations of the beginning and end of transition, since all the sensors seemed to be in between. At 47.4 million per foot, the end of transition appeared to be near 0.48 m for the 2 mm nose radius, and near 0.62 m for the 3 mm nose radius. At 12.6 million per foot, the beginning of transition was near 0.36 m for the 2 mm nose and 0.62 m for the 3 mm nose; the end of transition was near 0.6 m for the 2 mm nose. The sharp cone was turbulent for the two higher Reynolds numbers. The length of the transitional zone seemed to decrease dramatically when the nose bluntness increased into the region where roughness on the nose seemed to dominate transition. However, there is considerable uncertainty regarding the appropriate method of interpreting the data.

Recent VKI Measurements
of Roughness-Induced Transition

Carbonaro et al. have made several measurements of roughness-induced transition at hypersonic speeds on models at the Von Karman Institute tunnels in Belgium. See, for example, Refs. [92, 93, 94]. However, up to 1996 the measurements were made on sharp cones and flat plates, and compared with Bertin's Shuttle-based approach [95]. Carbonaro et al. were not able to trigger transition using roughness elements on the blunt face of a hemispherical model [92, p. 2A-13], probably because the Reynolds numbers in the VKI tunnels are too small.

Ref. [96] reports additional measurements on blunt bodies at Mach 6, in support of tripping efforts for the Atmospheric Reentry Demonstrator, a very blunt Apollo-like shape. The measurements were performed in a 6-inch Mach-6 open-jet tunnel at freestream Reynolds numbers of $8 - 20 \times 10^6$/m. Hemisphere-cylinders and blunt sphere-cones were studied, all had a nose radius of 20 mm. Distributed roughness was applied by knurling, and

isolated roughness was also tested in the form of spheres. Large isolated roughness heights k were needed to trip the flow, with $k/\delta^\star$ of 1-5 being correlated against $Re_e(x_{tr} - x_{sphere})/M_e^2$. Here, x_{sphere} appears to be the arclength from the nose to the location of the tripping sphere, but the symbols in Ref. [96] are not all defined. Distributed roughness was more effective at tripping, but was only successful on the cylindrical portion of the hemisphere-cylinder. The data are limited and do not appear successful in tripping on the hemisphere itself, probably because the Reynolds numbers are too low ($Re_D \simeq 0.32 - 0.80 \times 10^6$.)

Ref. [97] describes measurements on the Expert reentry geometry in the H3 and Longshot tunnels at VKI. The Expert vehicle is a very blunt pyramidal shape; the geometry is not specified. It appears that the shape, which is roughly 50% blunt, was split in two lengthwise to enable starting a larger model. The model was about 24 cm long, the height across the half-base was about 16 cm or 18 cm, and the roughness elements were placed 44 or 118 mm from the nose. Measurements were made with an infrared camera in the H3 tunnel at Mach 6, using isolated roughness with six heights ranging from 0.1 to 0.98 mm. Transition was inferred from the infrared images, in a way which is not specified. The results were then compared to the PANT correlation, which was fairly successful for the Mach-6 data. A shuttle-type correlation was not successful. Data was obtained in the Longshot tunnel at Mach 15 and unit Reynolds numbers to 7.5 million per meter, but these data do not agree with the PANT correlation. The few details given are insufficient to enable reanalysis.

70-deg. Sphere-Cone at Mach 6 – Horvath 1996

Horvath et al. measured the near-wake flow on a blunt planetary-probe shape in the 20-inch Mach-6 tunnel at Langley [98]. The nose radius was 1.5 in. and the diameter of the model was 6 in. The model was fixed at zero AOA and tested at $Re_D = 0.5 - 4.0 \times 10^6$. For some of the tests, aluminum oxide grit of about 0.015-in. diameter was dispersed on the forebody stagnation region. The roughness-height to displacement thickness ratio is stated to vary from about 3 near the stagnation point to about 1.2 near the end of the grit at about 90% of the radius, but the Reynolds number at which this was estimated is not given. Heat-transfer distributions were inferred from coaxial thermocouples and thin films.

For the two higher Reynolds numbers of 2 and 4 million, the forebody boundary layer transitioned to turbulence. For the lower Reynolds number of 0.5 million, the boundary layer did not transition, and the heating returned to laminar levels as the flow expanded around the model shoulder. Although this paper is focused on the wake flow, the measurements on the blunt face are suggestive of the conditions necessary for obtaining transition, and might be worth reanalyzing.

Genesis Sample Return Capsule

Transition on the Genesis sample-return capsule was measured in a Mach-6 wind tunnel by Cheatwood et al. [99]; this work was inadvertently omitted from Ref. [9]. Cheatwood et al. measured transition induced by surface cavities in the 20-inch Mach-6 tunnel at Langley. Four models with diameters of 3, 4, 5, and 6-in. were used, but it appears that only the 6-in. models were used for the transition measurements. The circular cavities were placed at 40% and 70% of the distance from the stagnation point to the rim. At zero angle of attack, the smallest cavity did not trip the flow, but the larger cavities did. A preliminary correlation of the transition location was plotted using Re_θ vs. w/δ, where w is the cavity diameter and δ is the boundary-layer thickness.

The sample-return capsule reentered the atmosphere on 8 Sept. 2004. Although the parachute failed, much of the heatshield was recovered intact [100]. It appears that transition occurred in a wedge downstream of the penetration, leaving a discolored region on the heatshield. The spreading angle in the wake is about 4-5 deg., a value similar to that observed by Van Driest and Blumer behind spherical trips on a hemisphere at Mach 2 [75]. Navier-Stokes computations show that transition increases the heating rate by a factor of more than 2 [100].

Unfortunately, it appears that the in-flight roughness due to the molybdenum penetration is not known. If the in-flight roughness can be inferred using post-flight measurements of the recovered hardware, it might be useful to revisit this issue so the flight data can be used to help understand blunt-body transition induced by roughness and cavities.

Mars Science Laboratory

Transition on the Mars Science Laboratory (MSL) [101] was reviewed in Ref. [9]. Since the preparation of that paper, Refs. [102], [103], and [104] became available. Edquist et al. provide computations of the laminar and turbulent aeroheating [103]; the vehicle was designed for turbulent heating to the blunt face, and thrust-plume interference heating to the afterbody. The blunt-face

boundary layer is expected to become turbulent before peak heating. Transition to turbulence increases the computed smooth-wall non-ablating peak heating rate by a factor of 2.5.

Hollis and Collier report measurements on MSL in AEDC Tunnel 9 at high Reynolds numbers [104]. The measurements were made on 6-in.-dia. solid metal models in perfect-gas nitrogen at Mach 8 and 10 for unit Reynolds numbers from 1 to 49 million per foot. Heating and transition were inferred from flush-mounted thermocouples. Since the experiments were focused on turbulent heating, the transition data were not analyzed in detail.

Transition appeared to depend on Mach number, since at Mach 10 it began near 15 million per foot, while at Mach 8 it began near 8 million per foot. Since the noise level in Tunnel 9 does not change much between these two Mach numbers, the source of this dependence is unknown [105]. The surface finish of the model is not given; it seems possible that particulate impact increased the roughness during the initial runs at Mach 10, but no evidence of such an effect is evident in the repeated runs. It is also possible that the apparent difference is simply an artifact of the large changes in unit Reynolds number between runs. However, Figs. 21, 22, 25, and 26 in the reference suggest a Mach number effect in addition to the Reynolds number effect.

The flow was thought to be transitional if the heating levels were significantly above laminar computations, yet well below turbulent computations. Without measurements of the fluctuations in the boundary layer, this inference cannot be confirmed.

Hollis and Collier also report measurements in the 20-inch Mach-6 tunnel at Langley, using surface thermocouples in a metal model instead of the usual phosphor-coated ceramic model. Transition occurred much later on the metal model, suggesting a significant impact of the surface roughness of the phosphor coating. It would be very interesting to see an analysis of transition using the computations and measurements in these two tunnels.

Offset Hemisphere-Cylinder at Mach 9
Schrijer 2004

Schrijer et al. measured on a hemisphere-cylinder in a Mach-9 Ludwieg-tube wind tunnel using infrared thermography [106]. The freestream unit Reynolds number varied from $4 - 14 \times 10^6$/m. The hemisphere had a 5-cm radius and was offset from the cylindrical afterbody by a height h, which ranged from -3.2 to 3.2 mm. Distributed roughness and tripping wires were also applied to the model nose. The heat transfer increased with roughness height, although it's not clear from the short paper that turbulent heating was achieved, as opposed to disturbed laminar heating. The results were correlated using PANT, Re_k, and a Shuttle-type approach. The grit roughness correlates well but the step roughness does not. Few details are shown, so it would be impossible to reanalyze the data.

Ballistic-Range Measurements on Hemispheres
Reda 2007

Reda's work in the NOL and AEDC ballistic ranges was later continued at NASA Ames. The Ames range and a general review of range measurements of roughness-induced transition is reported in Ref. [107]. Additional measurements on POCO graphite are reported in Ref. [108]. Additional transition data were measured for both laminar-ablated and bead-blasted POCO graphite hemispheres. The bead-blasted models had nose radii of 0.375 and were flown near 12 kft/s at range pressures from 0.58 to 0.75 atm. The roughness was about 0.57 mils. The laminar-ablated models had nose radii of 0.75 inches and were flown near 14 kft/s at range pressures from 0.25 to 0.38 atm. Heating rates were imaged using an intensified CCD camera. Transition occurred on the noses, and was correlated with Re_k, along with previous data. For values of

$$0.5 \leq \frac{\rho_k u_k \bar{k}}{\rho_e u_e \theta} \leq 2.5,$$

transition was correlated at $\rho_k u_k \bar{k}/\mu_w = 250$. Here, ρ_k and u_k are density and velocity in the undisturbed boundary layer at the roughness height k, ρ_e and u_e are density and velocity at the boundary layer edge, μ_w is the viscosity at the wall, $\bar{k}$ is the average roughness height, and θ is the momentum thickness. For

$$\frac{\rho_k u_k \bar{k}}{\rho_e u_e \theta} < 0.5,$$

the flow was thought to be in the smooth-wall limit, where $\rho_e u_e \theta/\mu_w = 500$ at transition. This smooth-wall limit is not generally valid, for much larger values have sometimes been measured [10, 15], but it may be useful for preliminary design. For

$$\frac{\rho_k u_k \bar{k}}{\rho_e u_e \theta} > 2.5,$$

the flow was thought to be in a large-roughness limit at low Reynolds number, where transition was expected at $\rho_e u_e \theta/\mu_w = 100$. It would be interesting

to see if the proposed large-roughness limit was consistently valid for measurements at other conditions and in other facilities.

Supersonic Measurements on Orion
Murphy et al. 2007

Murphy et al. measured aerodynamic forces on the Orion vehicle in the Unitary Plan tunnel at NASA Langley [109]. The 3.03% model was 6 in. in diameter and was tested mostly at a unit Reynolds number of 3×10^6/ft. for Mach numbers from 1.6 to 4.0. Angle of attack varied from 10 to 30 deg. Transition was inferred from qualitative images of heat transfer obtained using temperature-sensitive paint and an infrared camera.

For $Re_D = 1.5 \times 10^6$, at Mach 1.6, 2.0, and 2.5, the smooth model appeared to be laminar. At $Re_D = 2.5 - 3.5 \times 10^6$ and Mach 1.6, the flow was transitional, with streaks of turbulence emanating from probable roughness in the nominally smooth wall (the surface finish was not given.) Distributed roughness was applied in a narrow strip around the stagnation point, with roughness height varying from 0.005 to 0.012 in. The roughness height was determined using a simple analysis based on Ref. [110]. The trips were successful in generating a turbulent flow. The blunt face of the 'smooth' model became pitted during tunnel operation, due to the impact of particulate; these pits were also able to trip the flow [109, Fig. 16].

Dynamic stability is an issue for Orion development; it is very difficult to compute, due to the sensitivity of the moment coefficients to small errors [111]. Although Ref. [111] does not discuss the effect of transition on these moments, Ref. [112] showed that transition had a large effect on these moments for the Mercury spacecraft [9]. However, Ref. [109] shows that transition has little effect on the Orion moments at supersonic speeds, perhaps because Orion does not have the extended afterbody that Mercury and Gemini did.

Discussion

Laminar-turbulent transition on blunt geometries occurs when the Reynolds number is high enough, given a geometry, surface roughness, Mach number, stagnation enthalpy, wall temperature, tunnel noise level, angle of attack, and so on. For nominally smooth models, Reynolds numbers based on freestream conditions and diameter must be several million or more. For models with roughness typical of flight, Reynolds numbers must still be of the order of a million or more. It is difficult to reach these high Reynolds numbers in most facilities, since blunt models must be relatively small in order to permit successful starting of the tunnel. Thus, experimental data for blunt-body transition are rare and expensive to obtain. Accurate and reliable prediction of roughness-induced transition on blunt bodies remains a topic for future research.

Considerable data exists for the Apollo vehicle using various configurations of protuberances and trips. Given the cost of acquiring more data of this type, it would seem to be cost-effective to reanalyze this data to determine the conditions under which the roughness induced transition. Such computations could also be compared to more recent measurements.

Acknowledgements

Much of the work of developing this review was funded by the Northrop-Grumman Corporation, as preparation for the development of the Orion vehicle. The author's research has been funded by AFOSR, Sandia Nat'l Laboratory, NASA Johnson, NASA Langley, and NASA's Constellation University Institutes Project.

References

[1] William S. Saric. Görtler vortices. *Annual Review of Fluid Mechanics*, 26:379–409, 1994.

[2] L. M. Mack. Boundary layer linear stability theory. In *Report 709, Special Course on Stability and Transition of Laminar Flow*, pages 1–81. AGARD, March 1984.

[3] W.S. Saric, H.L. Reed, and E.B. White. Stability and transition of three-dimensional boundary layers. *Annual Review of Fluid Mechanics*, 35:413–440, 2003.

[4] D. Arnal and G. Casalis. Laminar-turbulent transition prediction in three-dimensional flows. *Progress in Aerospace Sciences*, 36(2):173–191, February 2000.

[5] Ira H. Abbott. Some factors contributing to scale effect at supersonic speeds. Memorandum AG4/M4, AGARD, September 1953. From the London AGARD Conference. NASA STI citation 68N83131.

[6] Steven P. Schneider. Effects of high-speed tunnel noise on laminar-turbulent transition. *Journal of Spacecraft and Rockets*, 38(3):323–333, May–June 2001.

[7] Matthew P. Borg, Steven P. Schneider, and Thomas J. Juliano. Effect of freestream noise on roughness-induced transition for the X-51A forebody. Paper 2008-0592, AIAA, January 2008.

[8] Steven P. Schneider. The development of hypersonic quiet tunnels. Paper 2007-4486, AIAA, June 2007. Revised version submitted to the J. Spacecraft and Rockets.

[9] Steven P. Schneider. Laminar-turbulent transition on reentry capsules and planetary probes. *Journal of Spacecraft and Rockets*, 43(6):1153–1173, Nov.-Dec. 2006. See erratum with correct color figures, v. 44, no. 2, pp. 464-484, March-April 2007.

[10] Steven P. Schneider. Flight data for boundary-layer transition at hypersonic and supersonic speeds. *Journal of Spacecraft and Rockets*, 36(1):8–20, 1999.

[11] Steven P. Schneider. Hypersonic laminar-turbulent transition on circular cones and scramjet forebodies. *Progress in Aerospace Sciences*, 40(1-2):1–50, 2004.

[12] Steven P. Schneider. Effects of roughness on hypersonic boundary-layer transition. Paper 2007-0305, AIAA, January 2007. Revised version to appear in the J. of Spacecraft and Rockets.

[13] Daniel C. Reda. Correlation of nosetip boundary-layer transition data measured in ballistics-range experiments. *AIAA Journal*, 19(3):329–339, March 1981.

[14] Daniel C. Reda. Review and synthesis of roughness-dominated transition correlations for reentry applications. *J. of Spacecraft and Rockets*, 39(2):161–167, March-April 2002.

[15] R. G. Batt and H.H. Legner. A review of roughness-induced nosetip transition. *AIAA Journal*, 21(1):7–22, January 1983.

[16] Scott Berry and Thomas Horvath. Discrete roughness transition for hypersonic flight vehicles. Paper 2007-0307, AIAA, January 2007.

[17] Steven P. Schneider. Laminar-turbulent transition on reentry capsules and planetary probes. Paper 2005-4763, AIAA, June 2005.

[18] North American Aviation. Experimental heat transfer and pressure distributions over entry configurations of 0.02-scale Apollo models H-1 and PS-1 and hemisphere-cylinders at Mach number of 10. Contractor Report NASA-CR-117543, SID-63-623, NASA, Jan. 1963. NASA STI citation 79N76090.

[19] G.L. Fox and J.G. Marvin. An investigation of the Apollo afterbody pressure and heat transfer at high enthalpy. Technical Memorandum NASA-TM-X-1197, NASA, March 1966.

[20] C.G. Miller III and P.L. Lawing. Experimental investigation of flow characteristics of the Apollo reentry configuration at a Mach number of 20 in nitrogen. Technical Memorandum NASA-TM-X-1258, NASA, July 1966.

[21] G. Lee and R.E. Sundell. Heat-transfer and pressure distributions on Apollo models at Mach 13.8 in an arc-heated wind tunnel. Technical Memorandum NASA-TM-X-1069, NASA, February 1965.

[22] George Lee and Robert E. Sundell. Apollo afterbody heat transfer and pressure with and without ablation at Mach 5.8 to 8.3. Technical Note NASA-TN-D-3620, NASA, September 1966.

[23] Joseph H. Kemp, Jr. Telemetry measurements of afterbody pressures on free-flying models of the Apollo capsule at Mach numbers from 10 to 21 in helium and 14 in air. Technical Memorandum NASA-TM-X-1154, NASA, October 1965.

[24] C.M. Akin. Experimental comparison of Apollo afterbody heating in air and carbon dioxide. Technical Memorandum NASA-TM-X-1204, NASA, January 1966.

[25] H. Gorowitz. NAA shock tunnel tests /ST-4/ of Apollo command modules H-6 and PS-6, data report, 2 May - 12 Jul. 1962. Contractor Report NASA-CR-117702, SID-62-1072, NASA, August 1962. NASA STI citation 79N76102.

[26] Charles E. DeRose. Trim attitude, lift and drag of the Apollo command module with offset center-of-gravity positions at Mach num-

bers to 29. Technical Note NASA-TN-D-5276, NASA, June 1969.

[27] R.I. Sammonds. Forces and moments on an Apollo model in air at Mach numbers to 35 and effects of changing face and corner radii. Technical Note NASA-TN-D-1086, NASA, April 1965.

[28] W.R. Lawrence and W. S. Norman. Free-flight range tests of the Apollo command module. Technical Report AEDC-TR-68-224, Arnold Engineering Development Center, January 1969. DTIC citation AD680396.

[29] John J. Bertin. The effect of protuberances, cavities, and angle of attack on the wind-tunnel pressure and heat-transfer distribution for the Apollo command module. Technical Memorandum NASA-TM-X-1243, NASA, October 1966.

[30] W.J. Biss and D.X. Emerson. Experimental heat transfer distributions over launch and entry configurations of an 0.045 scale Apollo model /H-2/ at Mach numbers of 8 and 10. Contractor Report NASA-CR-117538, SID-62-993-VOL1, NASA, Sept. 1962. NASA STI citation 79N76588. First of six volumes including appendices.

[31] R.X. Emerson. Experimental heat transfer distributions over the 0.090-scale Apollo command module /H-11/ with protuberances at Mach number 10. Contractor Report NASA-CR-117540, NASA, November 1964. NASA STI citation 79N76583.

[32] R.X. Emerson. Heat transfer tests of the 0.090-scale Apollo entry configuration /H-11/ in the AEDC-VKF hypersonic tunnel C. Contractor Report NASA-CR-154529, NASA, June 1964. NASA STI citation 78N70036.

[33] E.H. Fromm. Apollo model /H-1/ wind tunnel test /JPL 21-102/, volume 1 data report 16-26 April 1962. Contractor Report NASA-CR-117670, NASA, June 1962. NASA STI citation 79N76095. Note that the year shown in the STI citation is incorrect.

[34] E.H. Fromm. Apollo model /H-1/ wind tunnel test /JPL 21-102/, volume 2. Contractor Report NASA-CR-116724, NASA, June 1962. NASA STI citation 79N76373.

[35] Lester Lees. Laminar heat transfer over blunt-nosed bodies at hypersonic flight speeds. *Jet Propulsion*, 26:259–269, April 1956.

[36] Robert A. Jones and James L. Hunt. Effects of cavities, protuberances, and reaction-control jets on heat transfer to the Apollo command module. Technical Memorandum NASA-TM-X-1063, NASA, March 1965.

[37] James L. Hunt and Robert A. Jones. Effects of several ramp-fairing, umbilical, and pad configurations on aerodynamics heating to Apollo command module at Mach 8. Technical Memorandum NASA-TM-X-1640, NASA, September 1968.

[38] R.A. Jones and J.L. Hunt. Recent experimental studies on heat transfer to Apollo command module. In *Conference on Langley Research related to the Apollo mission*. NASA, January 1965. NASA STI citation 72N71555.

[39] North American Aviation. Apollo wind tunnel model nomenclature. Contractor Report NASA-CR-153876, NASA, July 1964. NASA STI citation 78N70030. SID-63-44-R-3, appears to be the 3rd revision. This appears to be the last available revision, for unknown reasons.

[40] North American Aviation. Apollo wind tunnel program report. Contractor Report NASA-CR-156432, SID-62-170-4, NASA, February 1963. NASA STI citation 78N75859. Note that the report date on the citation is incorrect. The report date from the title page is shown here.

[41] North American Aviation. Apollo wind tunnel program report. Contractor Report NASA-CR-156445, SID-62-170-5, NASA, July 1963. NASA STI citation 78N75635. This fifth revision appears to be the last available, for unknown reasons.

[42] G.A. Udvardy. Data report for experimental heat transfer distributions over launch and entry configurations on the 0.045-scale Apollo model /H-2/ with the addition of strakes at a Mach number of 10. Contractor Report NASA-CR-117230, SID-63-1135-VOL-1, NASA, Feb. 1964. NASA STI citation 79N76582. First of several volumes including appendices.

[43] North American Aviation. Experimental heat transfer distributions over launch and entry configurations on the 0.045-scale Apollo model /H-2/ with the addition of strakes at a Mach number of 10, volume 3. Contractor Report NASA-CR-116644, SID-63-1135-VOL-3, NASA, Feb. 1964. NASA STI citation 79N76578. Third of several volumes including appendices.

[44] North American Aviation. Experimental heat transfer distributions over launch and entry configurations on the 0.045-scale Apollo model /H-2/ with the addition of strakes at a Mach number of 10, volume 6. Contractor Report NASA-CR-116647, SID-63-1135-VOL-6, NASA, Feb. 1964. NASA STI citation 79N76579. Sixth of several volumes including appendices.

[45] W.J. Biss and D.X. Emerson. Experimental heat transfer distributions over launch and entry configurations of an 0.045 scale Apollo model /H-2/ at Mach numbers of 8 and 10. appendix A – plotted heat transfer distributions tunnel C, volume 3. Contractor Report NASA-CR-117551, SID-62-993-VOL-3-APP-A, NASA, Sept. 1962. NASA STI citation 79N76586. Third of six volumes including appendices.

[46] W.J. Biss and D.X. Emerson. Experimental heat transfer distributions over launch and entry configurations of an 0.045 scale Apollo model /H-2/ at Mach numbers of 8 and 10. volume 6, appendix B – tabulated data tunnel C. Contractor Report NASA-CR-117300, SID-62-993-VOL-6-APP-B, NASA, Sept. 1962. NASA STI citation 79N76590. Sixth of six volumes including appendices.

[47] W.J. Biss and D.X. Emerson. Experimental heat transfer distributions over launch and entry configurations of an 0.045 scale Apollo model /H-2/ at Mach numbers of 8 and 10. appendix A – plotted heat transfer distributions tunnel B, volume 2. Contractor Report NASA-CR-117542, SID-62-993-VOL-2-APP-A, NASA, Sept. 1962. NASA STI citation 79N76585. Second of six volumes including appendices.

[48] W.J. Biss and D.X. Emerson. Experimental heat transfer distributions over launch and entry configurations of an 0.045 scale Apollo model /H-2/ at Mach numbers of 8 and 10. appendix B – tabulated data tunnel B, volume 4. Contractor Report NASA-CR-117555, SID-62-993-VOL-4-APP-B, NASA, Sept. 1962. NASA STI citation 79N76587. Fourth of six volumes including appendices.

[49] W.J. Biss and D.X. Emerson. Experimental heat transfer distributions over launch and entry configurations of an 0.045 scale Apollo model /H-2/ at Mach numbers of 8 and 10. volume 5, appendix B – tabulated data tunnel B. Contractor Report NASA-CR-117297, SID-62-993-VOL-5-APP-B, NASA, Sept. 1962. NASA STI citation 79N76589. Fifth of six volumes including appendices.

[50] R. G. Batt and H.H. Legner. A review of roughness-induced nosetip transition. Paper 81-1223, AIAA, June 1981.

[51] M.R. Wool. Interim report, passive nosetip technology (PANT) program, volume X, Summary of experimental and analytical results (for the period May 1973 to December 1974). Technical Report TR-74-86-Vol-X, SAMSO, January 1975. Citation AD-A020708 in DTIC.

[52] M.J. Abbett, A.D. Anderson, L. Cooper, T.J. Dahm, J. Kelly, P. Overly, and S. Sandhu. Interim report, passive nosetip technology (PANT) program, volume XX, investigation of flow phenomena over reentry vehicle nosetips. Technical Report TR-74-86-Vol-XX, SAMSO, August 1975. Citation AD-A026617 in DTIC.

[53] M.D. Jackson. Interim report, passive nosetip technology (PANT) program, volume XV, roughness induced transition on blunt axisymmetric bodies – data report. Technical Report TR-74-86-Vol-XV, SAMSO, April 1974. Citation AD-A020713 in DTIC.

[54] R.M. Grabow and C.O. White. Surface roughness effects on nosetip ablation characteristics. Paper 74-513, AIAA, June 1974.

[55] D. A. Eitman and J. E. DeMichaels. Performance technology program (PTP-S II), Vol. X, material characterization of ground test models. Technical Report TR-80-40, BMO, January 1980. DTIC citation AD-A108849. An electronic copy with high-quality photographs is available from the Advanced Missile Signature Center, Missile Defense Agency, Arnold Engineering Development Center, Tullahoma, TN.

[56] Mark V. Morkovin. Bypass transition to turbulence and research desiderata. In *Transition in Turbines*, pages 161–199, May 1984. NASA CP-2386.

[57] Mark V. Morkovin. Critical evaluation of transition from laminar to turbulent shear layers with emphasis on hypersonically traveling bodies. Technical Report AFFDL-TR-68-149, Air Force Flight Dynamics Laboratory, 1969. DTIC citation AD-686178.

[58] Kenneth F. Stetson. Boundary-layer transition on blunt configurations. Technical Report JSC-26528, NASA Johnson Space Center, February 1994. An internal JSC report which should be available from the library. Prepared for Lockheed Engineering and Sciences Co., Report LESC-31143.

[59] J.D. Murphy and M.W. Rubesin. Re-evaluation of heat-transfer data obtained in flight tests of heat-sink shielded re-entry vehicles. *J. Spacecraft*, 3(1):53–60, January 1966.

[60] John D. Murphy and Morris W. Rubesin. An evaluation of free-flight test data for aerodynamic heating from laminar, turbulent, and transitional boundary layers. Part II – the X-17 re-entry body. Technical Report CR-70931, NASA, April 1965. Citation 66N20084 in RECON.

[61] E.J. Balgeman, G. Cassell, M.R. Dension, and D.M. Tellep. X-17 re-entry test vehicle: R-2 final flight report. Technical Report MSD-3003, Lockheed Aircraft Corp., April 1957. Citation 74N78004 in NASA RECON.

[62] Richard J. Wisniewski. Correlation of boundary-layer transition results on highly cooled blunt bodies. Technical Memorandum TM-X-412, NASA, October 1960.

[63] J. Leith Potter and Jack D. Whitfield. The relation between wall temperature and the effect of roughness on boundary-layer transition. *J. of Aero. Sci.*, 28(8):663–664, August 1961.

[64] M.L. Finson. Advanced reentry aeromechanics, interim scientific report, an analysis of nosetip boundary layer transition data. Report PSI-TR-52, Physical Sciences, Inc., August 1976. AFOSR-TR-76-1106.

[65] M.L. Finson, A.N. Pirri, P.E. Nebolsine, G.A. Simons, and P.K.S. Wu. Advanced reentry aeromechanics; final report. Report PSI-TR-115, Physical Sciences, Inc., January 1978. AFOSR-TR-78-0607TR, citation 78N25117 in NASA STI, citation AD-A052744 in DTIC.

[66] Alvin Seiff, Simon Sommer, and Thomas Canning. Some experiments at high supersonic speeds on the aerodynamic and boundary-layer transition characteristics of high-drag bodies of revolution. Research Memorandum RM-A56I05, NACA, January 1957. NASA STI citation 93R19613.

[67] Morton Cooper and Edward Mayo. Measurements of local heat transfer and pressure on six 2-inch-diameter blunt bodies at a Mach number of 4.95 and at Reynolds numbers per foot up to 81 x 10(exp 6). Memorandum NASA-MEMO-1-3-59L, NASA, March 1959. NASA STI citation 19980228467.

[68] Angelo Bandettini and Walter E. Isler. Boundary-layer transition measurements on hemispheres of various surface roughnesses in a wind tunnel at Mach numbers from 2.48 to 3.55. Memorandum NASA-MEMO-12-25-58A, NASA, March 1959. NASA STI citation 19980232078.

[69] Morton Cooper, Edward Mayo, and Jerome Julius. The influence of low wall temperature on boundary-layer transition and local heat transfer on 2-inch-diameter hemispheres at a Mach number of 4.95 and at a Reynolds numbers per foot of 73.2×10^6. Technical Note NASA-TN-D-391, NASA, July 1960. NASA STI citation 62N70965.

[70] K.F. Stetson. Nosetip bluntness effects on cone frustum boundary layer transition in hypersonic flow. Paper 83-1763, AIAA, July 1983.

[71] William D. Deveikis and Robert W. Walker. Local aerodynamic heat transfer and boundary-layer transition on roughened sphere-ellipsoid bodies at Mach number 3.0. Technical Report TN-D-907, NASA, August 1961.

[72] Mary W. Jackson and K.R. Czarnecki. Boundary-layer transition on a group of blunt nose shapes at a Mach number of 2.20. Technical Note TN-D-932, NASA, July 1961.

[73] James C. Dunavant and Howard W. Stone. Effect of roughness on heat transfer to hemisphere cylinders at Mach numbers 10.4 and

11.4. Technical Note TN-D-3871, NASA, March 1967.

[74] E.R. Van Driest, C.B. Blumer, and C.S. Wells, Jr. Boundary layer transition on blunt bodies – effects of roughness. *AIAA Journal*, 5:1913–1915, October 1967.

[75] E.R. Van Driest and C.B. Blumer. Boundary layer transition on cones and spheres at supersonic speeds – effects of roughness and cooling. Technical Report AFOSR-67-2048, North American Rockwell Corp, July 1967.

[76] R.L. Varwig. Effect of roughness on heating at the forward surface of a sphere at Mach 5. Report SAMSO-TR-70-229, Space and Missile Systems Organization, April 1970. Citation AD708471 in DTIC.

[77] D.H. Ross, J.W. Ellinwood, and R.L. Varwig. Hypersonic shock tunnel transition studies. In W. D. McCauley, editor, *Proceedings of the Boundary Layer Transition Workshop, Volume III*, December 1971. Paper 8 in the proceedings. Aerospace Corp. Report TOR-0172(S2816-16)-5, NASA citation 91N71710.

[78] Jack D. Coats. Investigation of the effects of nose bluntness on natural and induced boundary-layer transition on axisymmetric bodies in supersonic flow. Technical Report AEDC-TR-73-36, Arnold Engineering Development Center, February 1973. DTIC citation AD-755843.

[79] Theodore R. Creel, Jr. Experimental investigation at Mach 8 of the effects of projections and cavities on heat transfer to a model of the Viking aeroshell. Technical Memorandum TM-X-2941, NASA, April 1974.

[80] A.J. Laderman. Effect of surface roughness on blunt body boundary-layer transition. *J. of Spacecraft and Rockets*, 14(4):253–255, April 1977.

[81] A. Demetriades, A.J. Laderman, L. Von Seggern, A. T. Hopkins, and J. C. Donaldson. Effect of mass addition on the boundary layer of a hemisphere at Mach 6. *J. of Spacecraft and Rockets*, 13(8):508–509, August 1976.

[82] B.E. Richards and V. DiCristina. Heat transfer studies on ablation protected nosetips at reentry simulated conditions. Paper 77-781, AIAA, June 1977.

[83] Daniel C. Reda. Boundary-layer transition experiments on sharp, slender cones in supersonic free flight. *AIAA Journal*, 17(8):803–810, August 1979.

[84] Daniel C. Reda. Comparative transition performance of several nosetip materials at defined by ballistics-range testing. In *Proceedings of the 25th International Instrumentation Symposium held May 7-10, 1979, Anaheim, California*, pages 89–104, May 1979. See also the journal version in ISA Transactions, vol. 19, no. 1, Jan. 1980, pp. 83-98.

[85] A. Todisco, B. Reeves, D. Siegelman, and R. Mascola. Boundary layer transition on blunt axisymmetric nosetips induced by single and multiple craters. Paper 81-1087, AIAA, June 1981.

[86] A.T. Wassel, W.C.L. Shih, and J.F. Courtney. Roughness induced transition and heat transfer augmentation in hypersonic environments. Paper 84-0631, AIAA, March 1984.

[87] Henning Schöler. Thermal imaging on missiles in hypersonic flow. In *Missile Aerodynamics*, April 1990. AGARD CP-493, Paper 29.

[88] M.S. Holden. Studies of potential fluid-mechanical mechanisms for enhanced stagnation-point heating. In James N. Moss and Carl D. Scott, editors, *Thermophysical aspects of reentry flows*, pages 281–309. AIAA, New York, 1986. Vol. 103 in the series Progress in Astronautics and Aeronautics.

[89] Michael S. Holden and Kathleen M. Rodriguez. Studies of shock/shock interaction on smooth and transpiration-cooled hemispherical nosetips in hypersonic flows. Technical Report Report 7931, Calspan, April 1992. NASA Contractor Report CR-189585. NASA STI citation 92N33824.

[90] M.A. Zanchetta and R. Hillier. Laminar turbulent transition at hypersonic speeds: the effects of nose blunting. In *2nd European Symposium on aerothermodynamics for space vehicles*, pages 207–212. European Space Agency, February 1995. NASA STI citation 95N34688.

[91] Marcantony Zanchetta. *Kinetic heating and transition studies at hypersonic speeds*. PhD thesis, Department of Aeronautics, Imperial College of Science, Technology, and Medicine, London, England, April 1996.

[92] M. Carbonaro, J.-M. Charbonnier, and H. Deconinck. Hypersonic aerothermodynamics at VKI. In *Aerothermodynamics and propulsion integration for hypersonic vehicles*. AGARD, October 1996. AGARD-R-813, NASA STI citation 97N14778.

[93] J.-M. Charbonnier and H. Boerrigter. Roughness-induced transition in hypersonic flow. In *Space Scientific Research in Belgium, Vol. 4*, pages 43–44, March 1996. NASA STI citation 97N13183.

[94] H. Boerrigter and J.-M. Charbonnier. Roughness-induced transition in hypersonic flow. In *Space Scientific Research in Belgium, Vol. 4*, pages 51–52, March 1996. NASA STI citation 97N13186.

[95] J.J. Bertin, K.S. Stetson, S. A. Bouslog, and J.M. Caram. Effects of isolated roughness elements on boundary-layer transition for shuttle orbiter. *J. of Spacecraft and Rockets*, 34(4):426–436, July-August 1997.

[96] J.-M. Charbonnier, W. Dieudonne, and H. Boerrigter. Simulation of transitional and turbulent boundary layer flow on blunted geometry in hypersonic flow. In *3rd European Symposium on aerothermodynamics for space vehicles (ESTEC)*, pages 291–297. European Space Agency, November 1998. VKI reprint 1999-09, NASA STI citation 20000005304.

[97] S. Paris, D. Fletcher, L. Cerignat, and A. Garzon. Roughness-induced transition for flight experiments. In *Fourth International Symposium on Atmospheric Reentry Vehicles and Systems*, Arcachon, France, March 2005.

[98] Thomas J. Horvath, Catherine B. McGinley, and Klaus Hannemann. Blunt body near-wake flow field at Mach 6. Paper 96-1935, AIAA, June 1996.

[99] F. M. Cheatwood, N. R. Merski, C.J. Riley, and R.A. Mitcheltree. Aerothermodynamic environment definition for the Genesis sample return capsule. Paper 2001-2889, AIAA, June 2001.

[100] Chun Y. Tang and Michael J. Wright. Analysis of the forebody aeroheating environment during Genesis sample return capsule reentry. Paper 2007-1207, AIAA, January 2007.

[101] B.R. Hollis and D.S. Liechty. Boundary-layer transition correlations and aeroheating predictions for Mars Smart Lander. Paper 2002-2745, AIAA, June 2002.

[102] Karl T. Edquist, Derek S. Liechty, Brian R. Hollis, Stephen J. Alter, and Mark P. Loomis. Aeroheating environments for a Mars smart lander. *J. of Spacecraft and Rockets*, 43(2):330–339, March-April 2006.

[103] Karl T. Edquist, Artem A. Dyakonov, Micheal J. Wright, and Chun Y. Tang. Aerothermodynamic environments definition for the Mars Science Laboratory entry capsule. Paper 2007-1206, AIAA, January 2007.

[104] Brian R. Hollis and Arnold S. Collier. Turbulent aeroheating testing of Mars Science Laboratory entry vehicle in perfect-gas nitrogen. Paper 2007-1208, AIAA, January 2007.

[105] John F. Lafferty and Joseph D. Norris. Measurements of fluctuating pitot pressure, 'tunnel noise', in the AEDC hypervelocity wind tunnel no. 9. Paper 2007-1678, AIAA, February 2007.

[106] F.F.J. Schrijer, F. Scarano, B.W. Van Oudheusden, and W.J. Bannink. Experiments on hypersonic roughness induced transition by means of infrared thermography. In *5th European Symposium on aerothermodynamics for space vehicles*, pages 255–260. European Space Agency, November 2004. NASA STI citation 20050213395. Obtained from the Delft University website.

[107] D.C. Reda, M.C. Wilder, D.W. Bogdanoff, and J. Olejniczak. Aerothermodynamic testing of ablative reentry vehicle nosetip materials in hypersonic ballistic-range environments. Paper 2004-6829, AIAA, November 2004.

[108] D.C. Reda, M.C. Wilder, D.W. Bogdanoff, and D. Prabhu. Transition experiments on blunt bodies with distributed roughness in hypersonic free flight. Paper 2007-0306, AIAA, January 2007.

[109] Kelly J. Murphy, Stephen E. Borg, Anthony N. Watkins, Daniel R. Cole, and Richard J. Schwartz. Testing of the crew exploration vehicle in NASA Langley's unitary plan wind tunnel. Paper 2007-1005, AIAA, January 2007.

[110] Albert L. Braslow, Raymond M. Hicks, and Roy V. Harris, Jr. Use of grit-type boundary-layer transition trips on wind-tunnel models. Technical Note TN-D-3579, NASA, September 1966.

[111] James C. Ross. Aerodynamic testing in support of Orion spacecraft development. Paper 2007-1004, AIAA, January 2007.

[112] Simon C. Sommer, Barbara J. Short, and Dale L. Compton. Free-flight measurements of static and dynamic stability of models of the project Mercury re-entry capsule at Mach numbers 3 and 9.5. Technical Memorandum TM-X-373, NASA, August 1960.